CIVIL ENGINEERING STUDIES

STRUCTURAL RESEARCH SERIES NO. 100

THE RESPONSE OF BEAM-COLUMNS SUBJECTED TO DYNAMIC LATERAL LOADS

By
R. F. WOJCIESZAK
and
F. L. HOWLAND

Approved by
N. M. NEWMARK

Technical Report
to
WRIGHT AIR DEVELOPMENT CENTER
UNITED STATES AIR FORCE
Contract No. AF 33(616)-170
Expenditure Order No. R 449-37 AW-7

UNIVERSITY OF ILLINOIS
URBANA, ILLINOIS

DISTRIBUTION LIST

Commander
Wright Air Development Center
Wright-Patterson AFB, Ohio
ATTN: WCRRN - Blast Effects Research (5)

The Chief
Armed Forces Special Weapons Project
Washington 25, D. C.
ATTN: Weapons Effects Division (1)

Director of Intelligence
Headquarters, USAF
Washington 25, D. C.
ATTN: Mr. R. G. Grassy - AFOIN-3B (1)

Commander
Wright-Air Development Center
Wright-Patterson AFB, Ohio
ATTN: Major Andrew Boreske, WCOES-2 (1)

Document Service Center (DSC)
U. B. Building
Dayton, Ohio (1)

Armour Research Foundation
35 W. 33rd Street
Chicago 16, Illinois
ATTN: Dr. S. J. Fraenkel (1)

Drexel Institute
Philadelphia, Pennsylvania
ATTN: Professor Harry Bowman (1)

Massachusetts Institute of Technology
Department of Civil and Sanitary Engineering
Room 1-232
Cambridge 39, Massachusetts
ATTN: Dr. Charles Norris (1)

American Machine and Foundry Co.
Mechanics Research Department
1104 S. Wabash Ave.
Chicago 5, Illinois
ATTN: Mr. J. E. Fitzgerald (1)

DISTRIBUTION LIST (Continued)

The Rand Corporation
1700 Main Street
Santa Monica, California
ATTN: Dr. Marc Peter (1)

Professor Lynn S. Beedle
Fritz Laboratory
Lehigh University
Bethlehem, Pennsylvania (1)

Professor Bruce G. Johnston
301 West Engineering Building
University of Michigan
Ann Arbor, Michigan (1)

Dean W. L. Everitt
University of Illinois (1)

Professor N. M. Newmark
University of Illinois (2)

Professor W. H. Munse
University of Illinois (1)

N. Brooks
Project Supervisor of AF 24994
University of Illinois (1)

J. M. Massard
Project Supervisor of NObs 62250
University of Illinois (1)

F. L. Howland
Project Supervisor (2)

Project Personnel (6)

Project Files (10)

Technical Report

to

Wright Air Development Center

United States Air Force

Contract No. AF 33(616)-170

Expenditure Order No. R 449-37 AW-7

THE RESPONSE OF BEAM-COLUMNS SUBJECTED TO DYNAMIC LATERAL LOADS

by

R. F. Wojcieszak

and

F. L. Howland

Approved by

N. M. Newmark

University of Illinois

Urbana, Illinois

June 1955

TABLE OF CONTENTS

TABLE OF CONTENTS (CONT'D.)

LIST OF TABLES

LIST OF FIGURES

LIST OF FIGURES, CONT'D.

LIST OF FIGURES, CONT'D.

ACKNOWLEDGMENT

This investigation was performed in the Engineering Experiment Station of the University of Illinois, Department of Civil Engineering as a part of a project sponsored by the Wright Air Development Center, Department of the Air Force, under Contract AF 33(616)-170.

The work constitutes a part of the structural research program of the Department of Civil Engineering under the general direction of N. M. Newmark, Research Professor of Structural Engineering. The research project is under the direct supervision of F. L. Howland, Research Associate in Civil Engineering.

The author wishes to thank Dr. N. M. Newmark, Research Professor of Structural Engineering, for his direction of the investigation; W. H. Munse, Research Associate Professor of Civil Engineering, for his many helpful suggestions, and F. L. Howland, Research Associate in Civil Engineering, for his encouragement and supervision during the conduct of this study.

Sincere thanks are also expressed to W. Egger, L. W. Heilmann, J. H. Sams and C. L. Wilkinson, Research Assistants in Civil Engineering, for their aid and suggestions throughout the investigation.

The recording instruments used in the investigation were assembled and operated by V. J. McDonald, Research Assistant Professor of Civil Engineering, and R. J. Craig, Senior Electronic Technician, whose help was invaluable during the investigation.

The author also wishes to acknowledge the assistance of R. J. Horn, W. G. Kilker and P. R. Rendone for their help in the reduction of the test results.

1. INTRODUCTION

1.1 Introductory Remarks

To design a structure properly, an engineer must know how the structure will respond to the loads for which the structure is intended. When the load is static, the response relationship for the structure can be obtained by use of various elastic and plastic theories which relate loads and deformations. However, if the load is dynamic, the resistance to be used in determining the response of the structure is questionable and apparently varies from the static resistance to a value about 50% greater than the static resistance.

The investigation reported herein is concerned with the dynamic response of a relatively simple structure, a pin-ended beam-column. It is felt that in order to understand the behavior of complicated structures the fundamental behavior of the components must first be known.

1.2 Object and Scope

The objective of this investigation was to evaluate the dynamic resistance of beam-columns subjected to lateral dynamic loads.

The investigation was performed by testing four beam-columns in a drop test machine. Two of the beams were tested in the strong direction of resistance while the other two were tested in the weak direction of resistance. Each test was performed by varying the heights of drop in an increasing manner. This permitted a study of the dynamic resistance of the beam-column with respect to variations of energy input.

A constant axial load together with the dynamic lateral load was used in tests of two beam-columns, one oriented in the strong direction of resistance and the other in the weak direction of resistance.

1.3 Notation

The following notation has been used in this report:

Cross Sectional Constants

A = the area of the cross-section

A_c = the area of the cross-section in compression

A_t = the area of the cross-section in tension

dA = an element of area

b = the width of flange

c = the half depth of cross-section

f = the flange thickness

w = the web thickness

y = the distance from the centroidal axis of the specimen to the element of area

I_{xx} = moment of inertia about the centerline of the cross-section in the strong direction

I_{yy} = moment of inertia about the centerline of the cross-section in the weak direction

Loads

T = the axial load

P = resistance load of structure

P_d = applied dynamic load

M = total bending moment on section

Stresses

σ = unit compressive or tensile stress on any fiber

σ_e = static yield stress of the material

σ_y = yield stress

E = modulus of elasticity

Strains

ϵ = total strain on any fibers

ϵ_e = yield strain of the material

ϵ_{sh} = strain at which strain hardening begins

Deflections

Δ_S = static deflection

Δ_D = dynamic deflection

Δ_e = static yield deflection

Δ_i = initial permanent set deflection

Δ_M = maximum test deflection

Δ_{TM} = total maximum test deflection

W = deflection at any point X along the beam

Lengths

L = length of member

X = distance along beam

Energies

I_A = actual energy input due to lateral load

I_T = energy input as obtained from theoretical static resistance curve

I_{cr} = critical value of energy input

1.4 Summary of Investigation

The investigation consisted of testing, in a drop test machine, four pin-ended beams with an effective span of 80 in. The beams were fabricated from 4 M 13.0 rolled sections which were normalized to obtain uniform material properties. One pair of the specimens was tested in the strong direction while the other pair was tested in the weak direction. One specimen in each group was subjected to a constant axial load in addition to the dynamic lateral load. A test consisted of several drops of a 500 lb. weight from increasing heights so as to vary the energy input. For each test, lateral load, deflected shape, strains and axial load, if present, were recorded as functions of time on magnetic oscillographs.

The test results showed plainly that increasing the height of drop increased the duration of the load, the amplitude of the load and the maximum deflection of the specimen. The results also indicate that, as noted in previous static tests,[1]* the axial load had a much greater influence in reducing the stiffness of the specimen tested in the weak direction than when tested in the strong direction. In general, the axial load did not appreciably effect the resistance of the strong direction specimen when the center deflection was less than three times the static yield deflection. However, when the deflection was greater than this the resistance of the axially loaded specimen

*Numbers in parenthesis refer to corresponding numbered entries in the Bibliography at the end of the report.

was considerably less than the resistance of the specimen without axial load. With the weak direction specimens the load resistance was greatly affected by the axial load when the deflection exceeded the static yield deflection.

The theoretical static resistance curves were determined so that a comparison could be drawn between them and the dynamic test results. The determination of the theoretical static resistance curves was based on an idealized average stress strain curve. From this idealized stress-strain relationship and elementary mechanics the moment-flexural strain curves and the theoretical static load-deflection curves were obtained. The methods used to determine these relationships are presented in section 4.

The dynamic load had the effect of raising the yield stress level of the specimens tested in the strong direction. The amount the yield stress level was raised varied directly with the energy input or height of drop. With the weak direction specimens the dynamic effect was only apparent when the weight was dropped from a height of 48 in. It is believed that the reason the dynamic effect was not noticed in the smaller heights of drop is the fact that the initial slope of the dynamic resistance curve was probably much less than the initial slope of the theoretical static resistance curve.(1) Therefore, the dynamic increase in resistance would not be revealed by energy considerations alone. When axial load was present the dynamic resistance curve was of a decaying nature for both strong and weak direction specimens. However, the rate of decay was greater for the weak direction specimen.

2. TEST SPECIMENS AND APPARATUS

2.1 Material Used

Four pin-ended beams were tested during this investigation. The specimens were 4 M 13.0 sections of A-7 steel that had been normalized to obtain uniform stress-strain characteristics throughout the cross-section of each specimen.

2.2 Identification System

Each specimen was marked for identification. The identification mark served for positive identification and also to specify the type of test performed. The identification marks used and their meaning with regard to the type of test performed are as follows:

40XD4M - dynamically loaded in the strong direction; no thrust

41XD4M - dynamically loaded in the strong direction; thrust present

40YD4M - dynamically loaded in the weak direction; no thrust

41YD4M - dynamically loaded in the weak direction; axial load present

2.3 Section Properties

Section properties of the specimen can be found in an AISC Handbook[2] but for convenience are summarized in Table 1 along with the values obtained by assuming the web and flange to be of constant thickness for ease in analysis.

2.4 Fabrication

Each specimen was obtained from a length of beam equal to approximately 90 in. From the center 10 in. portion of this 90 in. length, coupons were cut in order to obtain the mechanical properties of the section. Eight standard A.S.T.M.[3] 0.5 x 0.25 tension coupons with a 2 in. gage length were sawed from each 10 in. section and tested statically according to A.S.T.M. Specifications,[3] to obtain their stress-strain relationship. Since the results for the four sections were quite similar, as shown in Table 2, an average stress-strain curve for all of the specimens was used. For computational purposes the strain hardening portion of the stress-strain relationship, as can be seen in Fig. 1, has been linearized.

The two 40 in. lengths of beam were welded together to form the specimen. A stub formed from a 10 I 25.4 was welded to the center of the beam, as shown in Fig. 2, for the purposes of transmitting lateral load to the specimen and to simulate the conditions of a floor system framing into a column. This welded connection is probably stiffer than would be encountered in actual practice but was used to insure that failure occurred in the member and not in the connection.

Bearing blocks were welded on each end of the specimen as can be seen in Fig. 3, to provide a pin-ended support when connected to the end reaction system. The specimen was supported in the end reaction system by means of two 2-1/2 in. diameter steel pins about which the specimen rotated. Needle bearings were used at the supports so that the friction encountered during rotation would be reduced to a minimum.

Each pin was held by two 1 in. x 9 in. steel plates, as can be seen in Figs. 4 and 5, which are free to translate when the dynamic load is applied. The translation is made possible by mounting the end plates with a nest of fourteen 1/4 in. diameter rollers placed on the top and bottom of each plate. The nests of rollers, in turn, ride in steel slots provided in the base plate and in the uplift restraint device which can be seen in Fig. 6.

2.5 Testing Apparatus

The apparatus used to test the two pin-ended specimens without axial load was a drop test machine which dropped a 500 lb. weight a preset height. A dynamometer placed between the specimen and the 500 lb. weight was used to measure the lateral load.

The tests with axial load required, in addition to the drop test machine, a hydraulic jack, and a spring and tie rod system.

The hydraulic jack was placed between one end of the specimen and the "U" frame of the tie rod system, as shown in Fig. 7. The "U" frame was constructed so that when the jack was in place the assembly would be in balance about the support pin. The axial load was applied to the specimen through the reaction system shown in Fig. 8.

A spring was placed between the other end of the specimen and the "U" frame, as shown in Fig. 9. This "U" frame also was constructed so that its balance point, with the spring in place, would be approximately at the support pin. The spring's purpose was to provide added flexibility to the tie rod system and maintain the axial load at a fairly constant

level during the test. The spring's reaction was transmitted to the specimen by means of the reaction system shown in Fig. 10.

The tie rod system included two tie rods, one on each side of the beam, which tied the two "U" frames together as can be seen in Fig. 11. A dynamometer, placed in each of the tie rods as shown in Fig. 12, permitted the determination of axial load.

2.6 Instrumentation

In these tests the deflections, applied lateral load, axial load, when present, and the maximum fiber strains at various sections along the length of the beam were recorded as functions of time on magnetic oscillographs. A diagram of the load and strain recording system is shown in Fig. 13. The lateral load dynamometer was an axially-loaded steel cylinder in which the load was measured by means of an SR-4 strain indicating bridge located near the end of the tube. The effective strain obtained from the bridge output was related to the load on the dynamometer by means of static load calibrations in which a relationship between static load and the effective strain, as measured by bridge output, was determined. This procedure and equipment had been developed in a previous study.(4)

The maximum fiber strains were measured at five locations along the length of the beam. These locations were 2-1/2 in., 5 in., 7-1/2 in., 10 in. and 15 in. from the loading stub. At each location, for specimens tested in the strong direction, there were two strain gages, one on top of the beam and the other on the bottom of the beam. These two gages

formed the two active arms of a four arm bridge whose output was proportional to the flexural strain. Flexural strain by definition is the average of the absolute values of compressive and tensile strain at the extreme fibers of the cross section.

At each location, for specimens tested in the weak direction, there were four strain gages, two on the top of the beam and two on the bottom of the beam. These four gages formed the four active arms of a four arm bridge whose output was proportional to the flexural strain.

Deflections were measured at the center and quarter points for all specimens tested in the strong direction and at the center and three eights points for all specimens tested in the weak direction. Slide wire gages as shown in Fig. 14, were used to measure the deflections. The complete deflection recording system is shown schematically in Fig. 15.

The specimens with axial load had the same instrumentation as the ones without axial load plus two channels for recording the variation in the axial load. The axial load dynamometers are steel rods in which the load is measured by means of an SR-4 strain gage bridge on the rods. The effective strain obtained from the bridge output was related to the load on the dynamometer by means of static load calibrations in which a relationship between the static load and the effective strain, as measured by bridge output, was determined.

For all of the tests in interlocking timing system was used to provide a constant zero for the time scales and is shown diagramatically in Fig. 16. A time signal (400 cps or 500 cps) was recorded by one galvanometer in each oscillograph and the interlock was provided by a switch driven at synchronous speed which provided steps in the time trace.

Since the highest frequency appearing prominently in the test records was approximately 150 cps, about one-half of the upper frequency limit of the recording equipment, it is believed that the test records obtained are essentially correct. Errors, in the final reduced test data or the possible percentage variations of this data from the measured maximum magnitude, result from reading and calibration of the various records. Repeated static calibrations of the load and deflection measuring instruments have indicated that the error in the static calibrations is probably less than 0.2 per cent of the load or deflection. The major source of error in the final results is probably associated with the measurement of the test records. For most of the traces obtained in these tests the reading errors in the load and deflection probably range from plus or minus 0.5 to 1 per cent of the maximum reported values. The smaller values correspond to the tests in which the deflections and loads were large and the larger errors are associated with the low energy input tests where the loads and deflections produced only small trace deflections. Since the loads and deflections were combined in the computation of the energy inputs the reported energy inputs may be from 1.0 to 2 per cent in error depending, as before, on the magnitude of the loads and deflections.

2.7 Test Procedure

The actual testing, whether axial load was present or not, was accomplished by dropping the 500 lb. weight from increasing preset heights. This was done to determine the effect of different energy inputs on the response of the specimens.

Before an actual test was made all circuits were checked and calibrations were run. Calibration of the lateral load, axial load and strain gage bridges consisted of shunting a known resistance across one arm of the bridge and actually obtaining a change in bridge output which was photographed on a section of the test record. Each shunting produced a different value of trace deflection which corresponded to a known value of load or strain. The deflection gages were calibrated by changing the bridge output to produce a trace deflection on the oscillograph record. The trace deflection was then related to the change in bridge output produced by a known static deflection.

Before and after each drop was made the traces were identified according to position on the record. This was done to insure that each trace could be identified when the data were reduced.

The oscillographs were turned on an instant before the weight was dropped and continued running until the weight had rebounded several times. However, only the record pertaining to the initial drop of the weight was used.

When axial load was present, a load of 35 kips was jacked on before the calibrations were run. The magnitude of the thrust was obtained by means of a portable strain indicator connected to the axial load dynamometers. During the dynamic test the change in the axial load was recorded.

3. TEST RESULTS

The test results of this investigation were interpreted in terms of the relationship between the maximum deflections and the energy input. This method of interpreting the test data provides at least qualitative if not quantitative comparisons between the static and dynamic resistances of the beam-columns.

3.1 Specimens 40XD4M and 41XD4M (Strong Direction)

Both specimens were tested by dropping the weight the same pre-determined heights. From the load-time curves and deflection-time curves of both specimens, as shown in Figs. 17 through 24, it can be seen that an increase in drop height produced an increase in amplitude and duration of lateral load and maximum deflection.

Comparing the test results by use of Table 3 and Figs. 17 through 24 one can see that in the small deflection range approximately from 0 to 3 times the elastic limit deflection, the response of the specimen, whether axial load was present or not, was essentially the same. This was concluded by observing that for the first two drops the maximum deflections were almost equal and the load-time curves and deflection time curves were almost identical. Since the energy input is approximately fixed by height of drop, Fig. 25 was plotted to show the maximum center deflection of the beams as a function of energy input. This figure reaffirms the previous conclusion about relatively small deflections.

It also can be seen in Fig. 25 that, for the specimen with axial load, the rate of change of energy input with respect to center deflection becomes smaller with increasing values of center deflection. This means that the lateral load or resistance decreases slightly with increasing values of center deflection.

The figure also shows that the resistance of the specimen without axial load increases with increasing values of center deflection. The increase in resistance function is caused by the presence of strain hardening.

3.2 Specimens 40YD4M and 41YD4M (Weak Direction)

There were four drops made on the specimen without axial load. Only the first two drops could be made on the specimen with axial load because the beam-column was on the verge of collapse after the 12 in. drop. The highest drop on the specimen without axial load was 48 in. This drop did not produce a failure in the member.

From the load-time relationships and the deflection-time relationships, as shown in Figs. 27 through 30, and as previously noted in the strong direction tests, an increase in drop height produced an increase in duration of load, amplitude of load and maximum deflection.

For each drop the energy input by the lateral load was obtained. The values of energy input and the maximum displacement for each drop can be seen in Table 4. From the values given in Table 4, Fig. 26 was obtained by plotting energy input vs. maximum center deflection for the

beam with axial load and the beam without axial load. From the figure one can conclude that the dynamic resistance function is approximately the same whether axial load is present or not up to a displacement of about the static yield deflection. As the center deflection increases the curves rapidly diverge. Following the reasoning used previously, this decreasing slope of the energy curve indicates the manner in which the resistance of the specimen with axial load decayed. A comparison of the rates of change of energy input for axially loaded specimens indicates when axial load is present the dynamic resistance of the specimen in the weak direction decays at a much greater rate than the dynamic resistance of the specimen in the strong direction.

4. DETERMINATION OF APPROXIMATE STATIC RESPONSE

The fundamental problem of the investigation is the correlation of the static resistance with the dynamic resistance of the specimen. In this section some approximate procedures will be presented for the determination of the static resistance of the beams whether axial load is present or not.

In general, before the static resistance can be determined a moment-flexural strain or moment-curvature relationship must be known.

4.1 Specimens Loaded in the Strong and Weak Directions; No Axial Load

The moment-extreme fiber strain relationship was determined using the average-idealized stress-strain curve shown in Fig. 1 and the equation:

$$M = \int_A \sigma y \, dA$$

where:

A is the area of the cross section of the specimen

dA is an element of area in the cross section of the specimen

y is the distance from the centroidal axis of the specimen to the element of area

σ is the unit stress acting on the element of area

The determination of a point on the moment-flexural strain curve was obtained by first choosing a value of flexural strain. Then the average stress-strain curve was used to determine the stress distribution across the specimen cross-section. The above equation integrated

numerically then yields the moment at the chosen value of flexural strain. The same procedure was followed for enough points so that a curve could be drawn that would represent the relationship between moment and flexural strain. The theoretical moment-flexural strain curves for 40XD4M and 40YD4M are shown in Figs. 31 and 32.

The static resistance was determined from the moment-flexural strain curve and the theory of small deflections. Using the theory of small deflections one can write the following differential equation:

$$\frac{d^2w}{dx^2} = (\pm \epsilon/c)_{T=0}$$

where:

ϵ is the extreme fiber strain

c is one-half of the depth of the specimen cross section

x is the coordinate along the length of the beam

w is the deflection

From the moment-flexural strain curve and using numerical procedures[5] or moment area theorems, the differential equation was solved for various values of maximum moment or maximum lateral load. The solution of the differential equation for a specified lateral load or moment is a point on the theoretical static resistance curve. The theoretical static resistance curves for 40XD4M and 40YD4M can be seen in Figs. 33 and 34.

4.2 Specimen Loaded in the Strong Direction; Axial Load Present

When an axial load is combined with the lateral load it is somewhat more difficult to obtain the moment-extreme fiber strain relationship. This relationship was obtained by use of the average idealized stress-strain curve and the equations:

$$M = \int_A \sigma y \, dA$$

$$T = \int_{A_c} \sigma \, dA - \int_{A_t} \sigma \, dA$$

where:

A_c is the area of the cross-section in compression

A_t is the area of the cross-section in tension

T is the axial load

A point on the moment-flexural strain curve was obtained by first choosing a value of extreme fiber strain at one extreme edge and then varying the extreme fiber strain at the other edge until the equation, $T = \int_{A_c} \sigma \, dA - \int_{A_t} \sigma \, dA$ was satisfied. With this strain distribution, the moment was computed using the procedure outlined in the previous section. The value of the flexural strain that was plotted with the moment was the average value of strain at the edges of the cross-section.

In order to obtain an approximate, theoretical static resistance an assumption was made as to the deflected shape of the specimen with axial and lateral load. It was assumed that the deflected shape of the

specimen with a lateral load, computed on the basis of the moment-flexural strain relationship which took account of the axial load, was identical to the actual deflected shape of the specimen with a combined lateral and axial load.

From the moment-flexural strain relationship for a given value of thrust, and the differential equation $\frac{d^2w}{dx^2} = (\pm \epsilon/c)_{T=T_1}$, a value of deflection, W_1, was obtained for an assumed moment diagram with the moment at midspan equal to M_1. This is shown in Fig. 35 as curve C_1. The assumed moment diagram had the same shape as the moment diagram for a simply supported beam with a concentrated load at midspan.

The assumption was then made that when an axial and lateral load acted simultaneously to produce a deflection, W_1, the moment at midspan would be equal to M_1. Therefore the moment due to lateral load only (curve C_1 - C_2 of Fig. 35), M_{L1}, is the difference between M_1 and the quantity, T_1W_1, represented by C_2 in Fig. 35. Since $M_{L1} = \frac{P_{L1}L}{4}$, where L is the length of the beam, the lateral load at a deflection of W_1 with an axial load T_1 acting, is .... $\frac{4}{L}(M_1 - T_1W_1)$ or $\frac{4}{L}(M_{L1})$.

The above procedure yields one point on the resistance curve when axial load is present. The theoretical resistance curves for specimen 41XD4M can be seen in Fig. 33.

4.3 Specimen Loaded in the Weak Direction; Axial Load Present

Since the axial loads that were used in this investigation do not appreciably change the position of the neutral axis from the centroidal axis; the moment-flexural strain curve, as Munz[6] has shown, is for all practical purposes the same whether axial load is present or not.

Therefore, using the same assumptions and procedures that were used for the specimen in the strong direction, the theoretical static resistance shown in Fig. 34 was obtained for a specimen with axial load.

5. CORRELATION OF TEST RESULTS WITH THE THEORETICAL STATIC RESPONSES

A correlation of the dynamic resistances with the theoretical static resistance of the beams was obtained by comparing actual energy input with the strain energy as predicted by the theoretical static resistance curve. The strain energy for a given value of deflection, W_1, by definition is the area under the load-deflection relationship from zero deflection to the deflection W_1.

The energy comparison is only valid at the time of maximum displacement when the kinetic energy is zero. This means that at the time of maximum displacement the energy input must equal the strain energy if energy losses are small in comparison with the total energy input.

5.1 Specimen 40XD4M

The actual energy input was greater than the theoretical static strain energy for every drop except the first one. The difference in behavior in the first drop could be because of the low energy input, and to stress concentrations and residual stresses which would tend to make the initial slope of the actual resistance curve less than the initial slope of the theoretical static resistance curve.(1)

With the other drops the theoretical static resistance was raised by using higher values of yield stress to produce response curves, as shown in Fig. 33, which provide a strain energy equal to the energy input. The raised response curves are assumed to be flat after yielding and until they reached the original theoretical static response curve

in the strain hardening region. The validity of the assumed shape of the resistance function is clearly shown by Wilkinson's[7] test results. Table 5 demonstrates that the amount the yield stress of the theoretical static resistance curve had to be raised to have the computed strain energy equal to the energy input increased with an increase in height of drop.

The dynamic resistance can also be correlated with the theoretical static resistance in terms of deflections. In this comparison, a value of Δ_S is determined by integrating the area under the theoretical static resistance curve, such that the theoretical static strain energy is made equal to the actual energy input. The value of Δ_S thus determined was always greater than the maximum dynamic displacement, Δ_D obtained in the tests. From this procedure, the curves shown in Fig. 36 were obtained. These curves represent the correlation of test results with the theoretical static relationships for all the drops except the first one. The two curves show also the effect of neglecting the permanent set, which increased after each drop due to inelastic damage, on the relationship between energy input and Δ_D/Δ_S. If the permanent set is neglected, the dynamic resistance of the specimen appears to be greater than it actually is.

This figure shows also that the deflection produced by the dynamic energy input was always less than the deflection to be expected from static energy input. In other words, a beam's capacity for energy absorption becomes greater under dynamic loads.

5.2 Specimen 41XD4M

From a comparison of the actual energy input with the strain energy computed from the theoretical static resistance curve, as shown in Table 6, it can be seen that the actual energy input was always greater than the strain energy. From this observation it can be concluded that for a dynamic lateral load the yield stress is apparently greater than the static yield stress.

The input energies from the dynamic lateral loads were approximately the same for the specimen with axial load, 41XD4M, as they were for 40XD4M since the heights of drop were approximately the same for each specimen. However, in addition to the energy from the lateral load, the axial load also supplied energy. This energy supplied by the axial load was in all cases equal to approximately twenty per cent of the total energy input. Thus, a difference in behavior might be expected in the two tests. However, by comparing the test results of specimens 40XD4M and 41XD4M, it was observed that resistances of the specimens were approximately the same as long as the deflection did not exceed approximately three times the static yield deflection. For the specimen without axial load, 40XD4M, it was found that the yield stress level varied with energy input. It would seem, therefore, that the increase in yield stress level depends upon the energy input provided by the dynamic lateral load and that the presence of the axial load does not have an appreciable effect on the yield stress level.

As noted earlier for each test of specimen 40XD4M a yield stress level was determined to provide agreement between the theoretical and measured energy input. These yield stress levels were then used for the corresponding heights of drop on specimen 41XD4M to obtain an upper bound of the load-deflection relationship for 41XD4M by the method described in section 4. This upper bound curve is represented by C_5 in Fig. 37.

When the deflections become large, as indicated by test results, the resistance decays. Just how the resistance decays is not completely understood but a lower bound of the resistance curve should be the theoretical static resistance curve. Since, for large deflections, the specimen is subjected to strain hardening which eliminates the increase in resistance brought about by the dynamic load.(8)

An attempt to obtain the qualitative shape of the resistance function for the specimen with axial load is shown in Fig. 37. The initial portion of this resistance curve is approximately the same as it would be for a beam without axial load as long as the deflections do not exceed three times the static yield deflection. The general shape of the decaying portion of the resistance curve was obtained by trial and error. The method consisted of assuming a general shape of resistance function and then checking to see if the strain energy as predicted by the assumed shape would equal the energy input. However, further study is required before more definite and complete information on the nature of the dynamic resistance can be presented.

5.3 Specimen 40YD4M

Specimens tested in the weak direction, as observed by Munz[6], are sensitive to stress concentrations and residual stresses. This would seem to explain why the actual energy inputs for the first three drops are less than those obtained by use of the theoretical static response. In the last drop the energy input was larger than the strain energy as determined from the theoretical static response curve. By raising the yield stress for the theoretical response curve, as previously mentioned, the strain energy can be made equal to the actual energy input. Table 7 compares the actual energy inputs for each drop with the strain energy obtained by the use of the theoretical static resistance curve with increased values of the yield stress.

5.4 Specimen 41YD4M

Comparing the actual energy inputs for specimen 41YD4m with the values obtained from the theoretical static response one finds that the actual inputs were always less than those obtained by using the theoretical static response. These differences could be due to stress concentrations and residual stresses which are thought to play an important part in determining the initial slope of the response curve. From Table 8, which summarizes the comparison between the test results and theory, an estimated qualitative resistance curve was drawn and is shown in Fig. 38.

6. SUMMARY AND CONCLUSIONS

From the test results and the theoretical static response curves the following statements can be made concerning the specimens tested dynamically in the strong direction:

1. The yield stress level was found to increase with an increase in energy input.
2. The axial load had very little effect on the response of the specimen in the small deflection range from approximately zero to three times the static yield deflection. For larger deflections the axial load had the effect of causing the response to decay toward the theoretical static response curve.
3. Further investigation is required to determine the resisting function more completely.

The following statements, which are based on the test results and the theoretical static curves, can be made about the specimens tested dynamically in the weak direction:

1. The dynamic resistance did not seem to be much greater than the theoretical static resistance.
2. After yielding the presence of axial load caused the dynamic resistance to decay to the theoretical static resistance for a beam with axial load.

3. The initial slope of the dynamic response curve is less than the theoretical static slope possibly because of the presence of stress concentrations and residual stresses.
4. Further investigation is still needed to determine more fully the fundamental behavior of the members.

BIBLIOGRAPHY

(1) Howland, F. L., Egger, W., Mayerjak, R. J. and Munz, R. J., "Static and Dynamic Load-Deflection Tests of Steel Structures" Civil Engineering Studies, Structural Research Series No. 92, University of Illinois.

(2) American Institute of Steel Construction, "Steel Construction Manual", New York, 5th Ed., (1951)

(3) American Society for Testing Materials, "ASTM Specifications for Rolled Structural Steel", Philadelphia, Pa., (1952).

(4) Howland, F. L., "The Development of an Apparatus for Applying Pulse Loads to Structures", M.S. Thesis, University of Illinois, (1952).

(5) Newmark, N. M., "Numerical Procedure for Computing Deflections, Moments, and Buckling Loads", Transactions of the ASCE, Vol. 108, pp. 1161-1234, (1945).

(6) Munz, R. J., "Static Tests to Failure of Steel Beam-Columns", M.S. Thesis, University of Illinois, Department of Civil Engineering, (1954).

(7) Wilkenson, C. L., "The Response of Model Frames Subjected to Dynamic Lateral Loads", M.S. Thesis, University of Illinois, Department of Civil Engineering, (1955).

(8) Nadai, A., "Theory of Flow and Fracture of Solids", Vol. 1, Second Edition, McGraw-Hill 1950.

TABLE 1

SUMMARY OF SECTION PROPERTIES

OF 4 M 13.0 SECTION

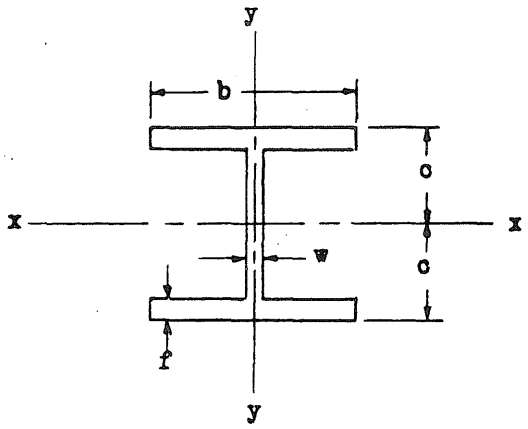

	Area	c	f	b	w	I_{xx}	I_{yy}
AISC Values	3.82	2.00	--	3.94	0.25	10.4	3.4
Idealized Values	3.77	2.00	0.375	3.94	0.25	10.4	3.8

TABLE 2

SUMMARY OF COUPON RESULTS USED IN THE
DETERMINATION OF THE IDEALIZED AVERAGE STRESS-STRAIN CURVE

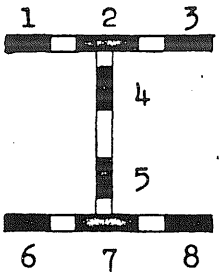

Specimen	Position	σ_e ksi	ϵ_e in/in	ϵ_{sh} in/in
40XD4M	1	36.32	0.001211	0.01396
	2	34.88	0.001163	0.01546
	3	36.21	0.001207	0.01133
	4	40.64	0.001355	---
	5	40.41	0.001347	0.01742
	6	35.71	0.001190	0.01577
	7	34.95	0.001165	0.01165
	8	35.94	0.001195	0.01165
Average		36.87	0.001229	0.01456
40YD4M	1	38.30	0.001227	0.01531
	2	32.41	0.001080	0.01058
	3	37.53	0.001251	0.01300
	4	40.32	0.001344	0.01776
	5	39.58	0.001329	0.01613
	6	35.45	0.001182	0.01318
	7	33.30	0.001110	0.01278
	8	35.86	0.001195	----
Average		36.63	0.001221	0.01411

TABLE 2 CONT'D

SUMMARY OF COUPON RESULTS USED IN THE
DETERMINATION OF THE IDEALIZED AVERAGE STRESS-STRAIN CURVE

Specimen	Position	σ_e ksi	ϵ_e in/in	ϵ_{sh} in/in
41XD4M	1	37.62	0.001224	0.01452
	2	35.86	0.001195	0.01494
	3	35.82	0.001194	0.01169
	4	41.31	0.001377	0.01649
	5	39.69	0.001323	0.01537
	6	35.82	0.001194	0.01234
	7	33.20	0.001107	0.01341
	8	35.19	0.001173	0.01215
Average		36.70	0.001223	0.01386
41YD4M	1	35.76	0.001192	0.01013
	2	35.37	0.001179	0.01575
	3	36.25	0.001208	0.01451
	4	40.36	0.001345	0.01965
	5	41.11	0.001370	0.02085
	6	36.01	0.001200	0.01475
	7	34.38	0.001146	0.01435
	8	37.42	0.001247	0.01680
Average		37.08	0.001236	0.01585
Overall Average		36.82	0.001227	0.01460

TABLE 3

COMPARISON OF TESTS 40XD4M
AND 41XD4M

Δ_e = 0.327 in.

SPECIMEN	DROP NO.	Δ_i in.	Δ_M in.	Δ_{TM} in.	$\frac{\Delta_M}{\Delta_e}$	$\frac{\Delta_{TM}}{\Delta_e}$	I_A in.-kips
40XD4M	1=12"	0	0.53	0.53	1.62	1.62	3.17
(34.13^K)* 41XD4M		0	0.55	0.55	1.68	1.68	3.33
40XD4M	2=24"	0.04	0.86	0.90	2.63	2.75	7.91
(33.31^K)* 41XD4M		0.04	0.91	0.95	2.78	2.91	8.46
40XD4M	3=48"	0.34	1.50	1.84	4.59	5.63	18.65
((29.58^K)* 41XD4M		0.45	1.84	2.29	5.63	7.00	19.80
40XD4M	4=72"	1.22	2.15	3.37	6.57	10.31	29.60
(23.85^K)* 41XD4M		1.83	2.67	4.50	8.17	13.76	29.65

*Indicates average value of thrust in kips.

TABLE 4

COMPARISON OF TESTS 40YD4M
AND 41YD4M

Δ_e = 0.332 in.

SPECIMEN	DROP NO.	Δ_i in.	Δ_M in.	Δ_{TM} in.	$\frac{\Delta_M}{\Delta_e}$	$\frac{\Delta_{TM}}{\Delta_e}$	I_A in.-kips
40YD4M	1=6"	0.00	0.82	0.82	2.47	2.47	2.46
(33.43K)* 41YD4M		0.00	1.02	1.02	3.07	3.07	2.42
40YD4M	2=12"	0.10	1.26	1.36	3.79	4.09	5.29
(27.07K)* 41YD4M		0.51	2.59	3.10	7.80	9.33	5.79**
40YD4M	3=24"	0.65	2.14	2.79	6.44	8.40	11.18
-----		----	----	----	----	----	----
40YD4M	4=48"	1.90	3.60	5.50	10.83	16.57	26.75
-----		----	----	----	----	----	-----

*Indicates average value of thrust in kips.

**This drop produced failure.

TABLE 5

COMPARISON OF TEST RESULTS OF 40XD4M WITH THEORETICAL STATIC RESPONSE

THEORETICAL STATIC YIELD DEFLECTION = 0.327 in.

DROP NO.	Δ_i	Δ_M	Δ_{TM}	I_A	I_T				
					$\sigma_y = \sigma_e$	$\sigma_y = 1.1\sigma_e$	$\sigma_y = 1.2\sigma_e$	$\sigma_y = 1.3\sigma_e$	$\sigma_y = 1.4\sigma_e$
	in.	in.	in.	in.-kips	in.-kips	in.-kips	in.-kips	in.-kips	in.-kips
1 = 12"	0	0.53	0.53	3.17	3.90	----	----	----	----
2 = 24"	0.04	0.86	0.90	7.91	7.60	8.24	----	----	----
3 = 48"	0.34	1.50	1.84	18.65	15.45	----	17.56	18.80	----
4 = 72"	1.22	2.15	3.37	29.60	----	----	----	28.34	29.96

TABLE 6

COMPARISON OF TEST RESULTS OF 41XD4M WITH THE THEORETICAL STATIC RESPONSE

DROP NO.	AVERAGE THRUST	Δ_1	I_A	Δ_M	Δ_{TM}	I_T
	kips	in.	in.-kips	in.	in.	in.-kips
1 = 12"	34.13	0	3.33	0.55	0.55	3.26
2 = 24"	33.31	0.04	8.46	0.91	0.95	6.21
3 = 48"	29.58	0.45	19.80	1.84	2.29	14.24
4 = 72"	23.85	1.83	29.65	2.67	4.50	22.66

TABLE 7

COMPARISON OF TEST RESULTS OF 40YD4M WITH THEORETICAL STATIC RESPONSE

Theoretical Static Yield Deflection = 0.332 in.

DROP NO.	Δ_i	Δ_M	Δ_{TM}	I_A	I_T					
					$\sigma_y = \sigma_e$	$\sigma_y = 1.1\sigma_e$	$\sigma_y = 1.2\sigma_e$	$\sigma_y = 1.3\sigma_e$	$\sigma_y = 1.4\sigma_e$	$\sigma_y = 1.5\sigma_e$
	in.	in.	in.	in.-kips	in.-kips	in-kips	in-kips	in.-kips	in-kips	in-kips
1 = 6"	0	0.82	0.82	2.46	3.07	----	----	----	----	----
2 = 12"	0.10	1.26	1.36	5.29	5.67	----	----	----	----	----
3 = 24"	0.65	2.14	2.79	11.18	11.21	----	----	----	----	----
4 = 48"	1.90	3.60	5.50	26.75	21.98	----	----	----	26.08	27.78

TABLE 8

COMPARISON OF TEST RESULTS OF 41YD4M WITH THE THEORETICAL STATIC RESPONSE

DROP NO.	AVERAGE THRUST	Δ_i	I_A	Δ_M	Δ_{TM}	I_T
	kips	in.	in.-kips	in.	in.	in.-kips
1 = 6"	33.43	0	2.42	1.02	1.02	3.38
2 = 12"	27.07	0.51	5.79	2.59	3.10	8.13

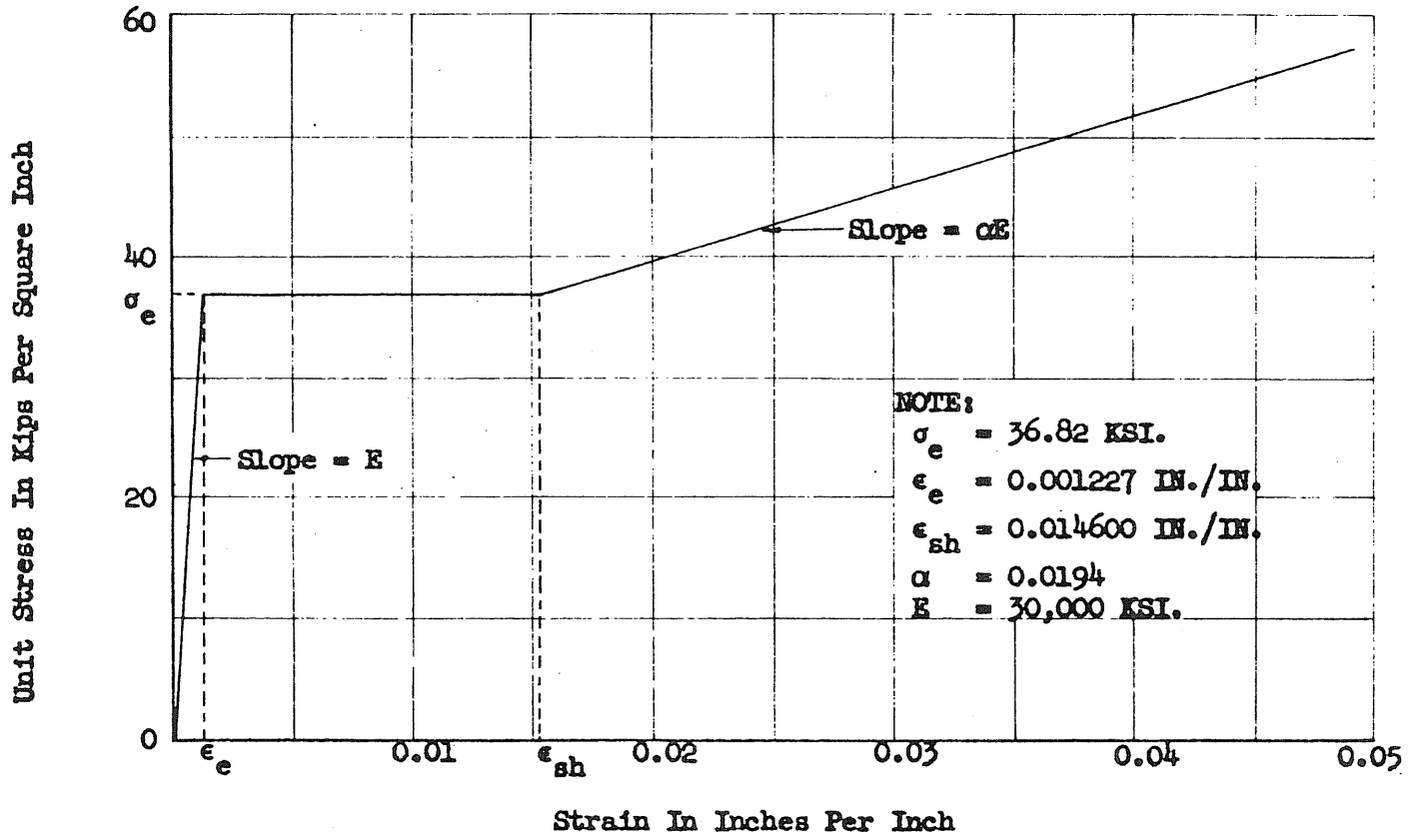

FIG. 1 IDEALIZED AVERAGE STRESS-STRAIN CURVE FOR ALL SPECIMENS TESTED

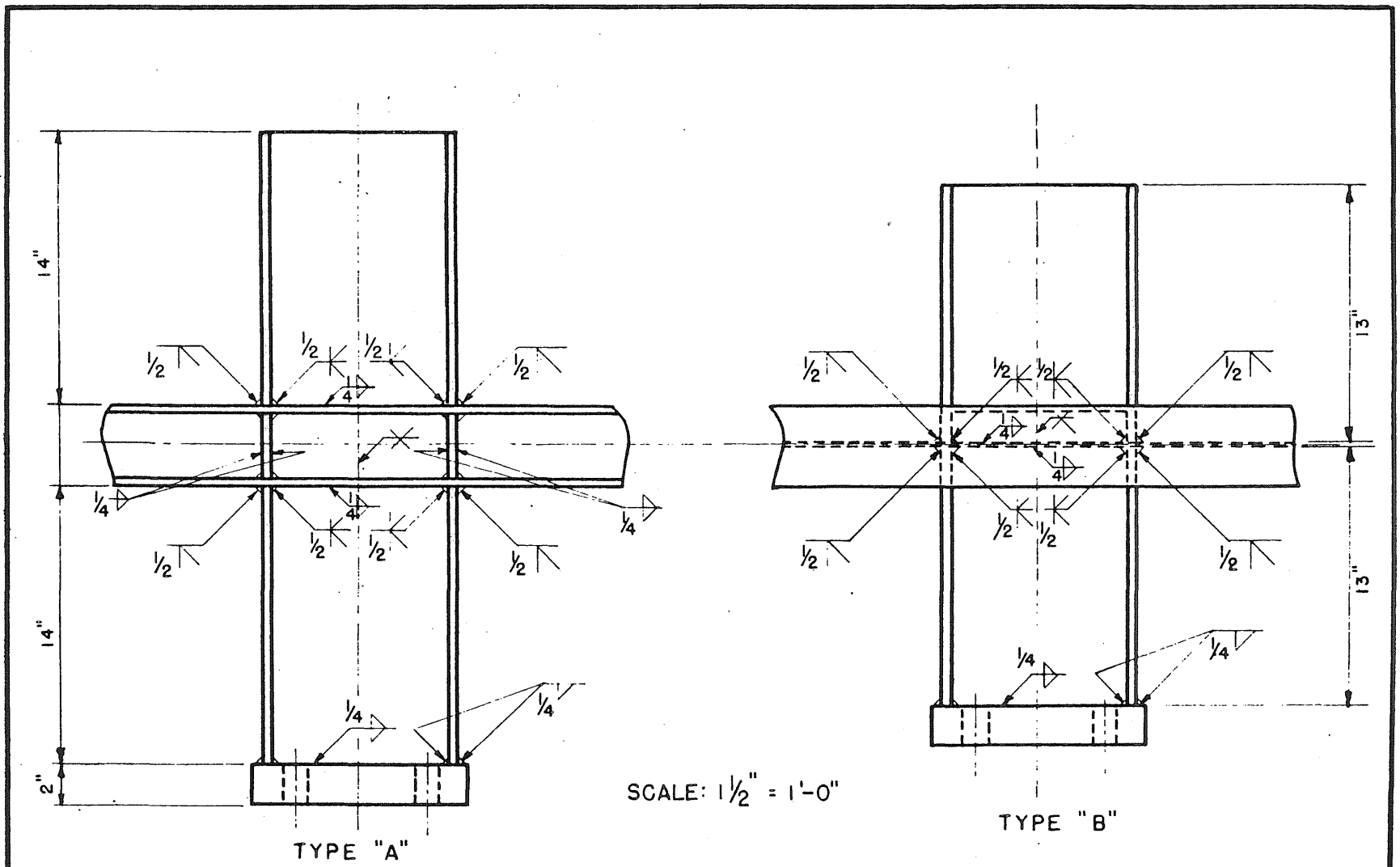

FIG. 2 STUB BEAM CONNECTION DETAILS

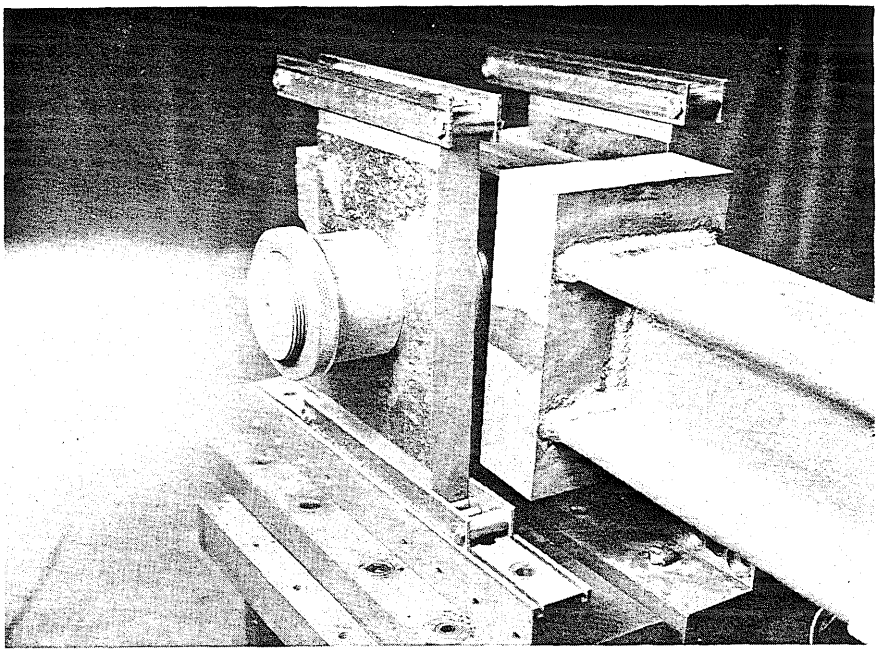

FIG. 3 WELDED CONNECTION BETWEEN SPECIMEN AND BEARING BLOCK

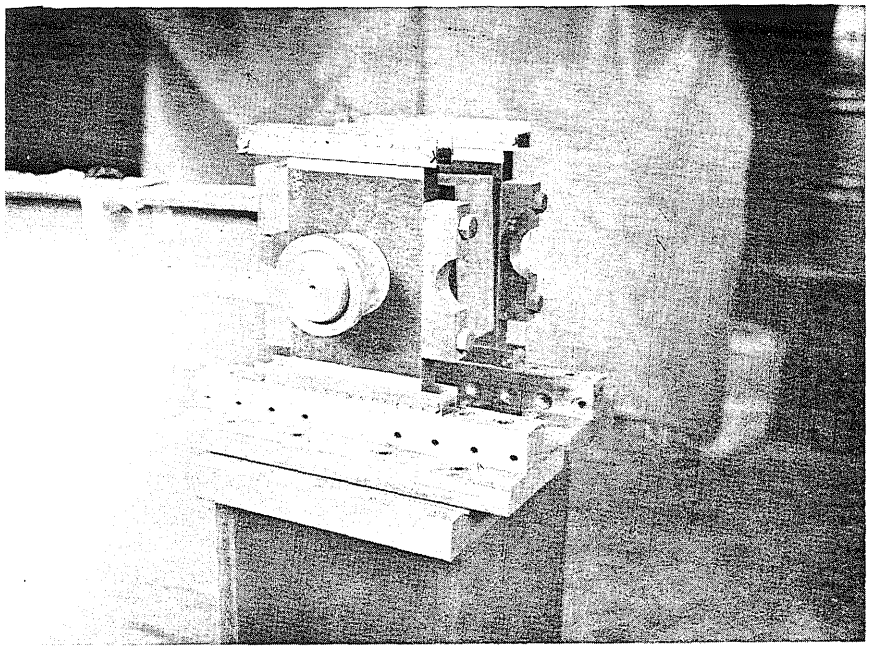

FIG. 4 SIDE VIEW OF END REACTION SYSTEM

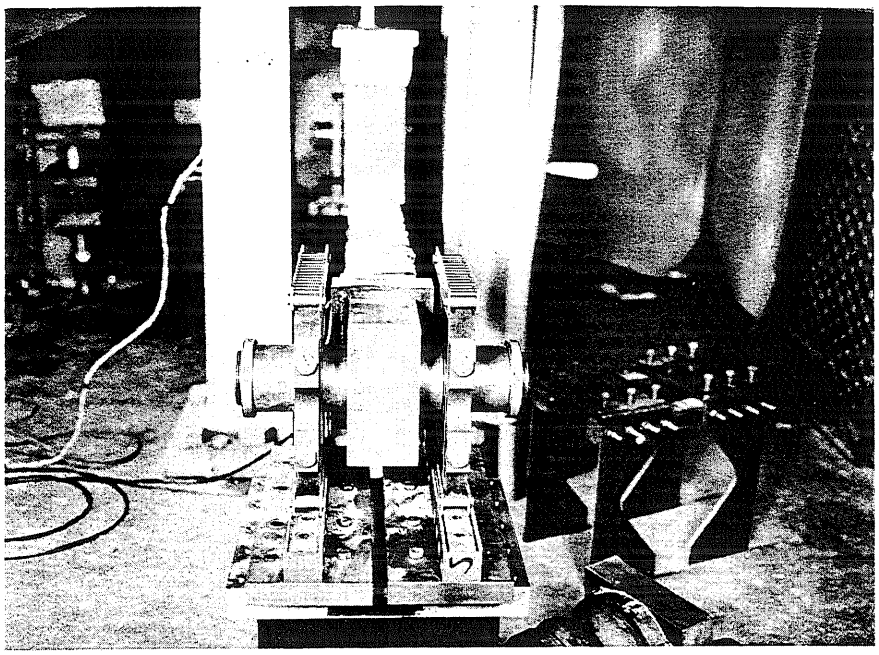

FIG. 5 END VIEW OF END REACTION SYSTEM

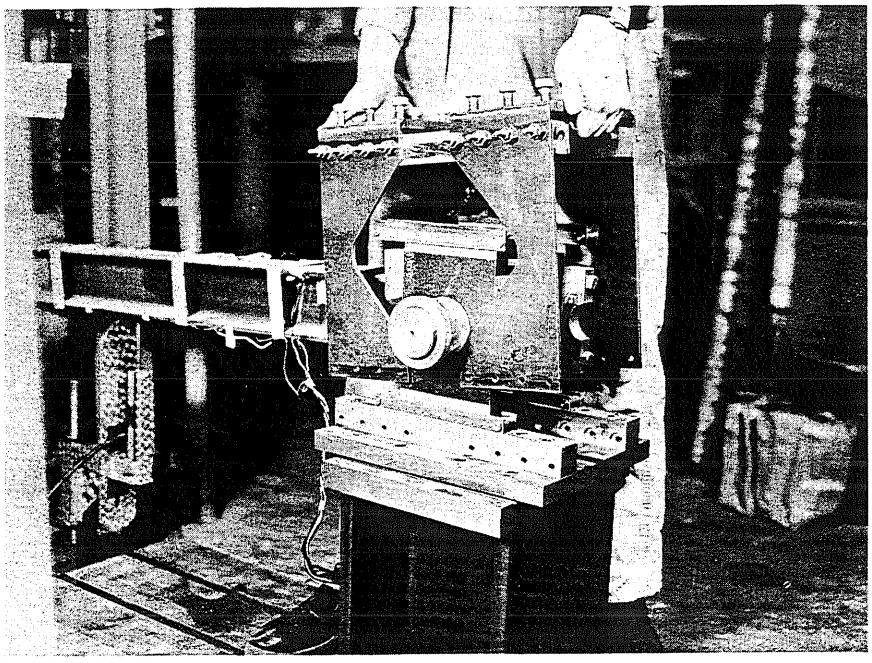

FIG. 6 END REACTION SYSTEM, UNLIFT RESTRAINT BEING PLACED

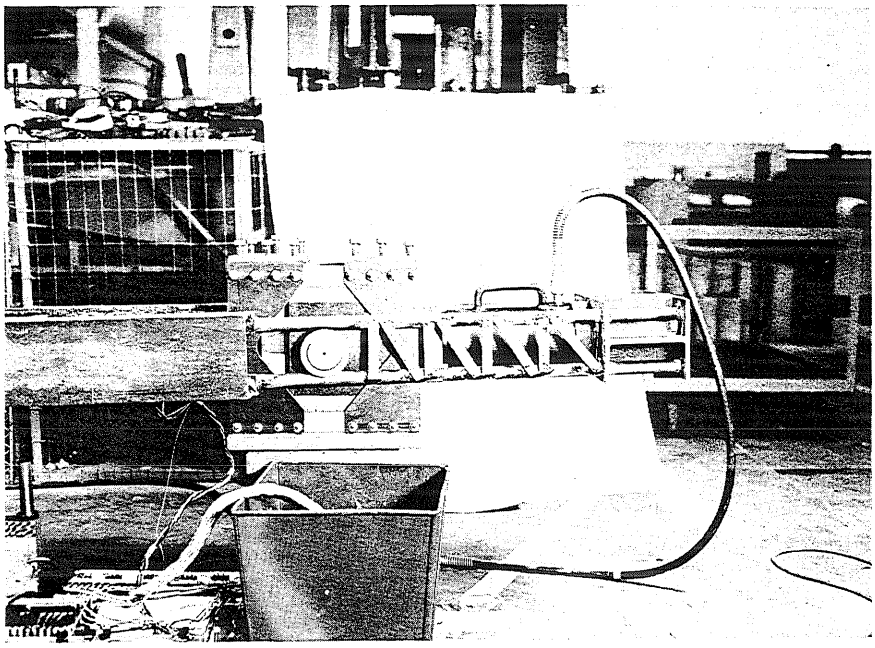

FIG. 7 WEST END REACTION SYSTEM WITH AXIAL LOAD PRESENT

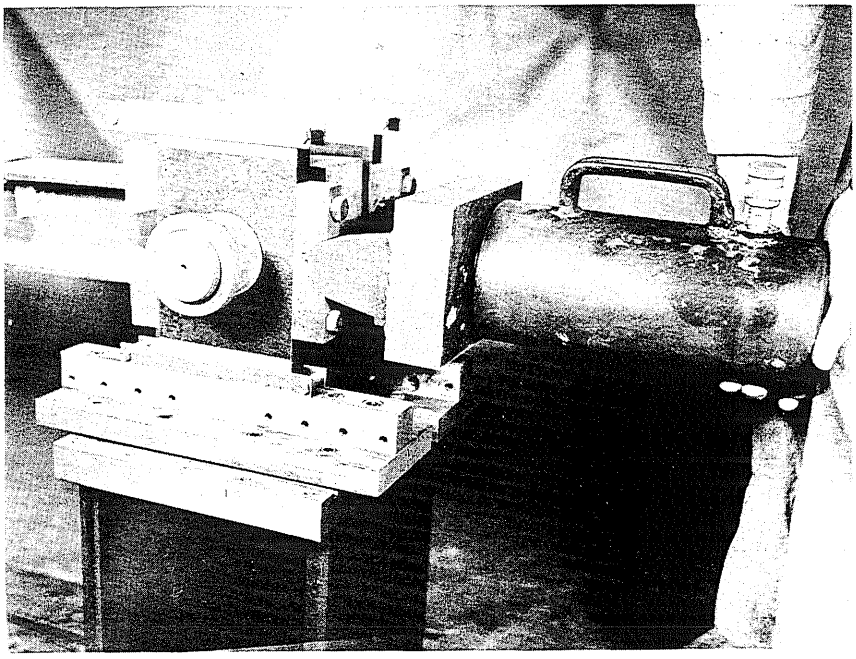

FIG. 8 AXIAL LOAD JACK

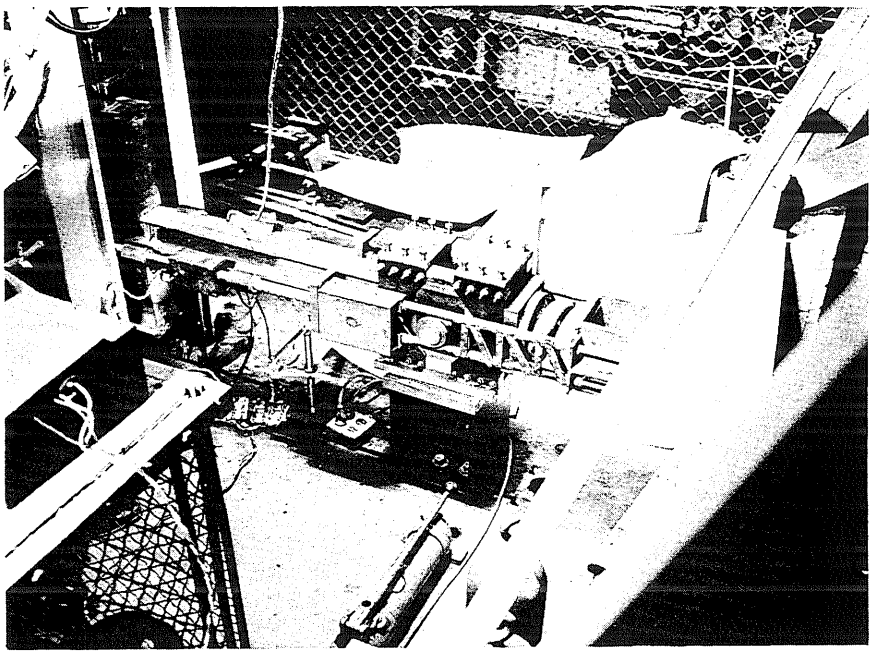

FIG. 9 EAST END REACTION SYSTEM WITH AXIAL LOAD PRESENT

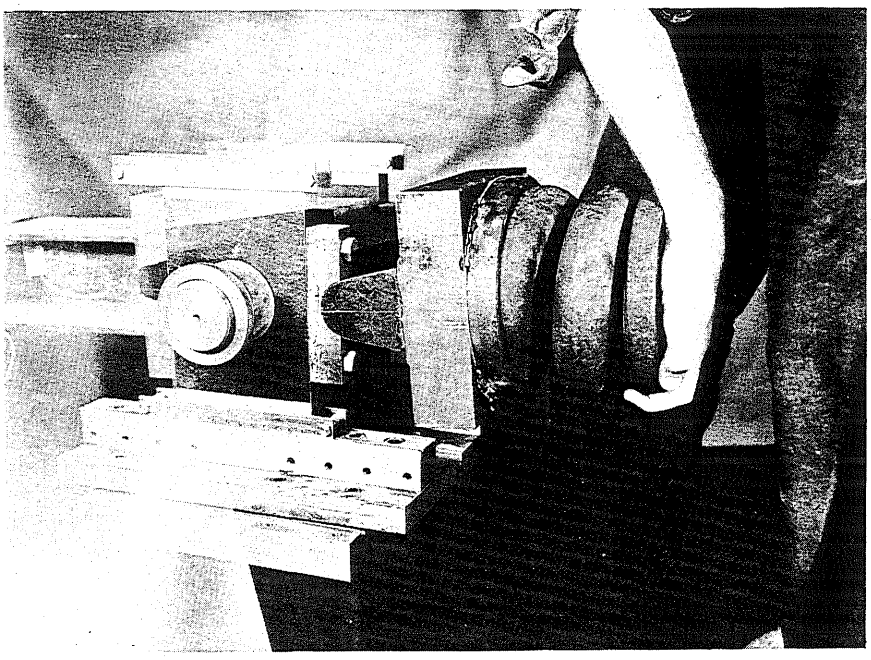

FIG. 10 SPRING REACTION FOR AXIAL LOAD SYSTEM

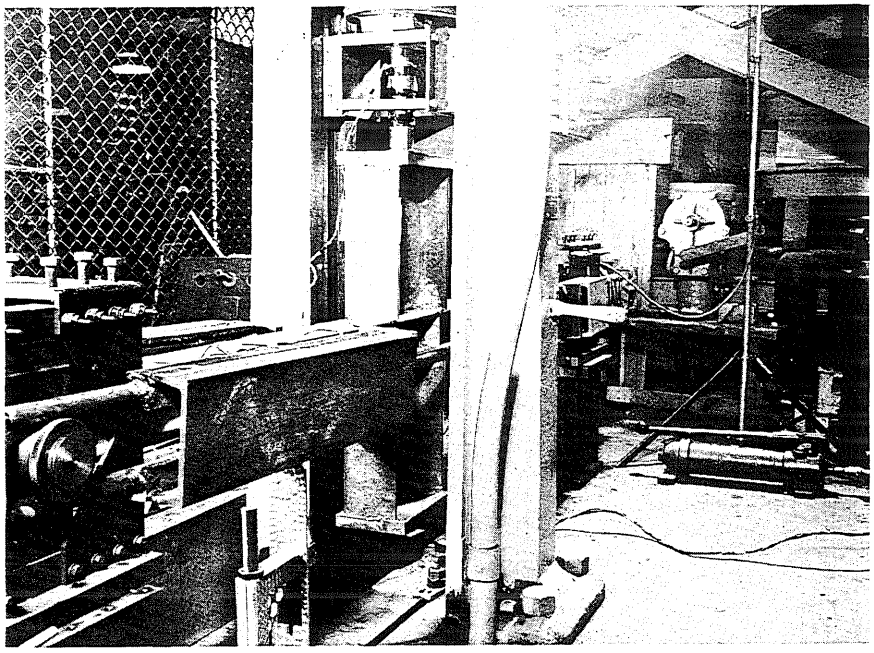

FIG. 11 AXIAL LOAD TIE ROD SYSTEM

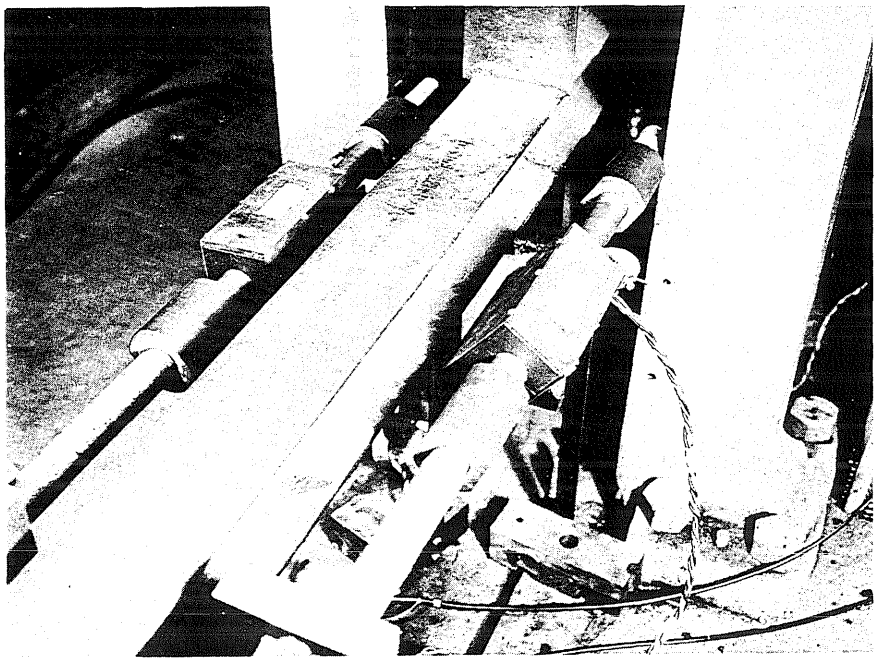

FIG. 12 AXIAL LOAD DYNAMOMETERS

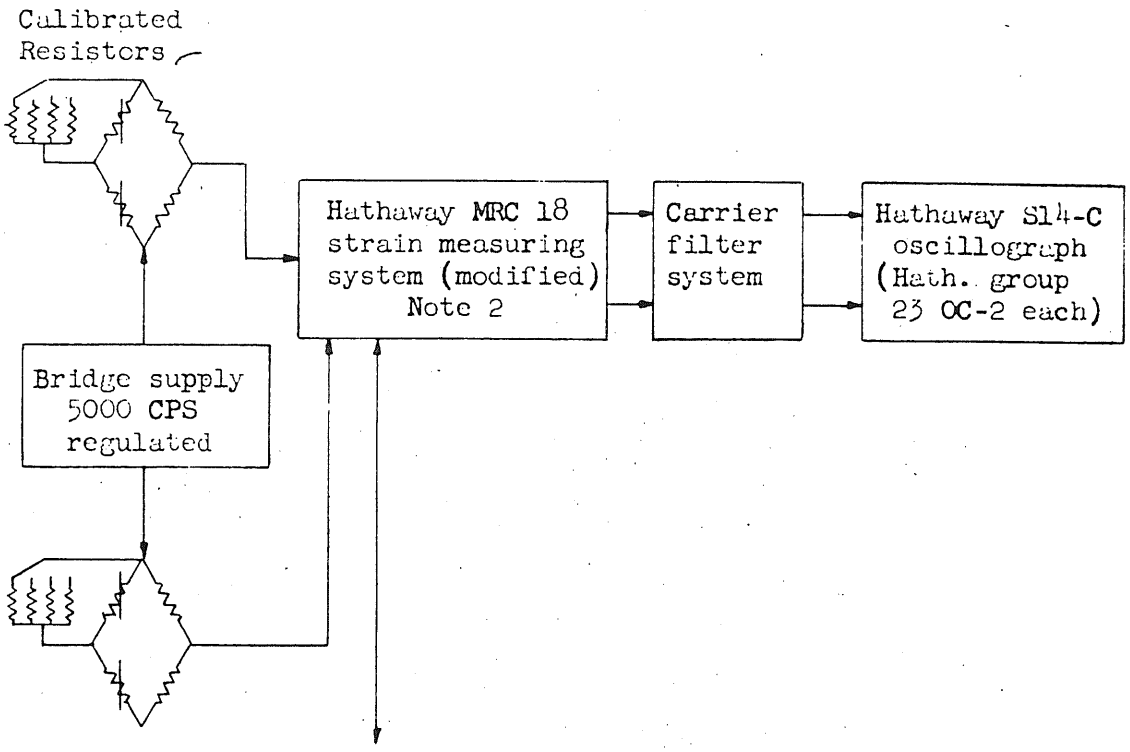

Note 1

Total of 6 to 8 channels of strain equipment used. (5 for strain measurements, 1 for lateral load measurement and 2 for axial load measurement, when present.)

Note 2

Standard Hathaway MRC 18 unit modified to reduce cross-talk between channels and to provide carrier supply oscillator with approximately 0.01% regulation.

FIG. 13 LOAD AND STRAIN MEASURING CHANNELS

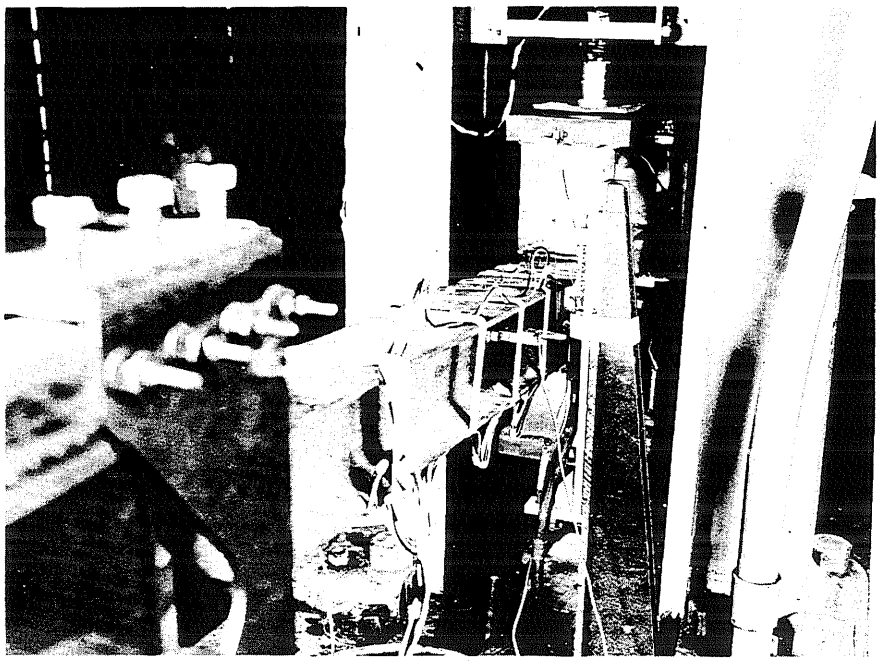

FIG. 14 SLIDE WIRE DEFLECTION GAGE

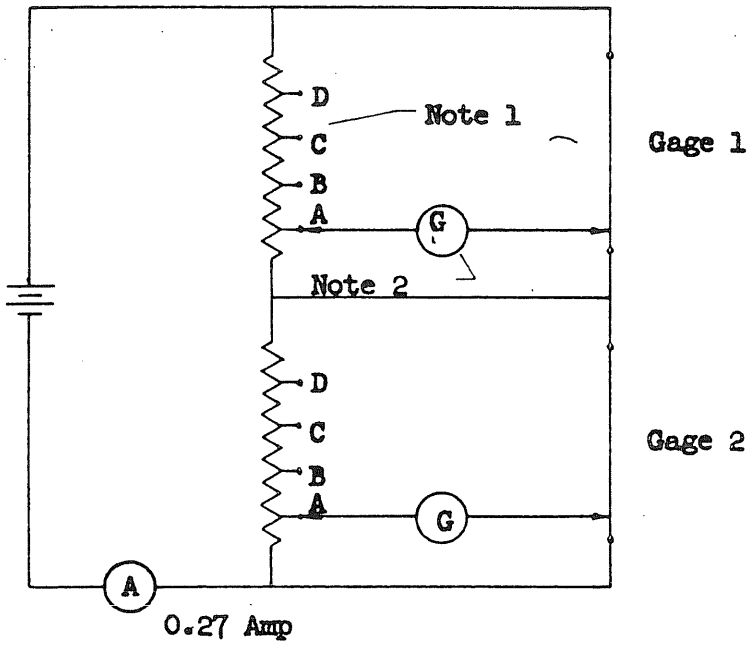

Note 1

Connections to B, C and D for calibration purposes. Nominal values; B = 0.5"; C = 2.0"; D = 4.0"; Precise values taken from gage calibration curves. "A" is the balance position at zero deflection.

Note 2

Recording Galvanometers are Hathaway Type OC2, Group 23 units used in Hathaway S14-C Magnetic Oscillographs.

FIG. 15 DEFLECTION GAGE SYSTEM

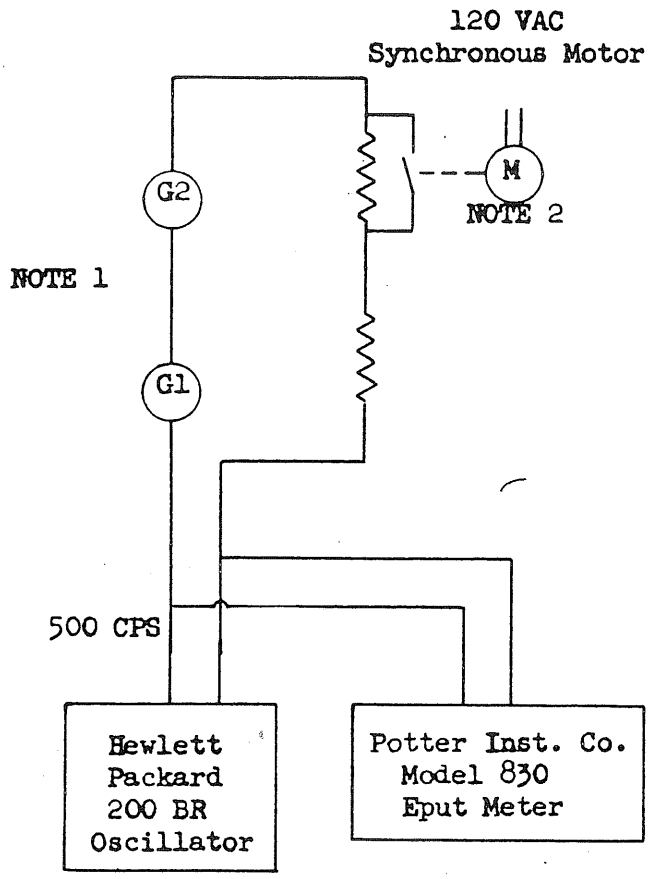

Note 1

G1 and G2 are Hathaway OC2 group 23 galvanometers. One galvanometer is located in each Hathaway S14-C oscillograph.

Note 2

Switch driven at synchronous speeds modulating the amplitude of the timing signal with steps every 0.02 min. and a step omitted once each 0.1 min.

FIG. 16 TIMING AND SYNCHRONIZING TRACES

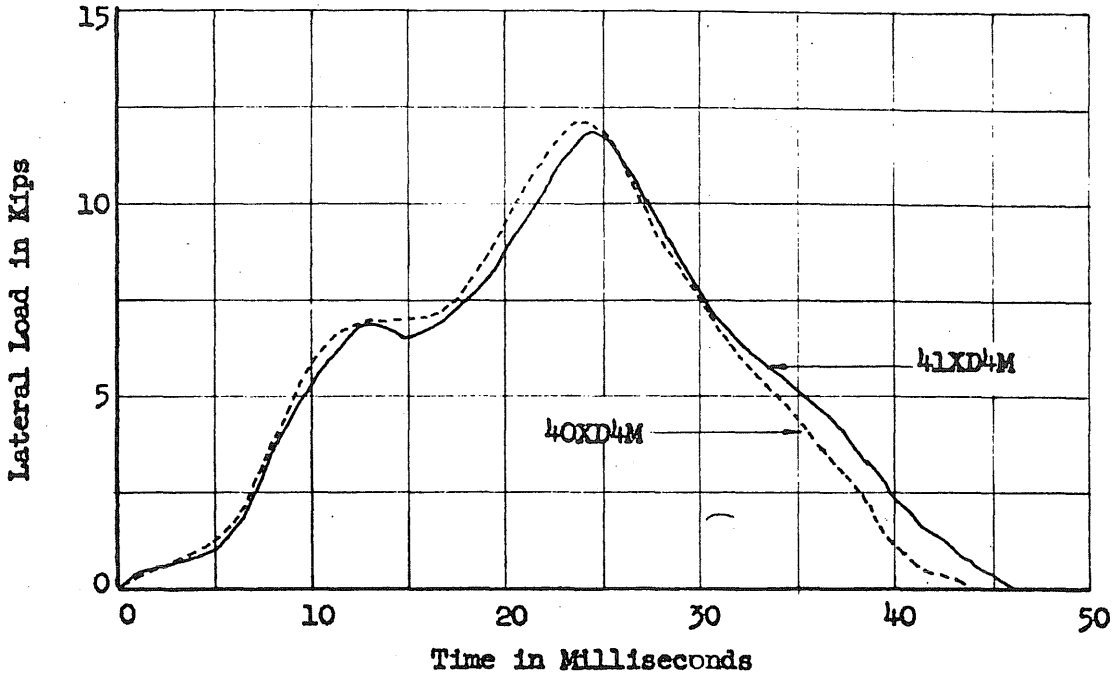

FIG. 17 LOAD-TIME RELATIONSHIP FOR STRONG DIRECTION SPECIMENS; HEIGHT OF DROP = 12 in.

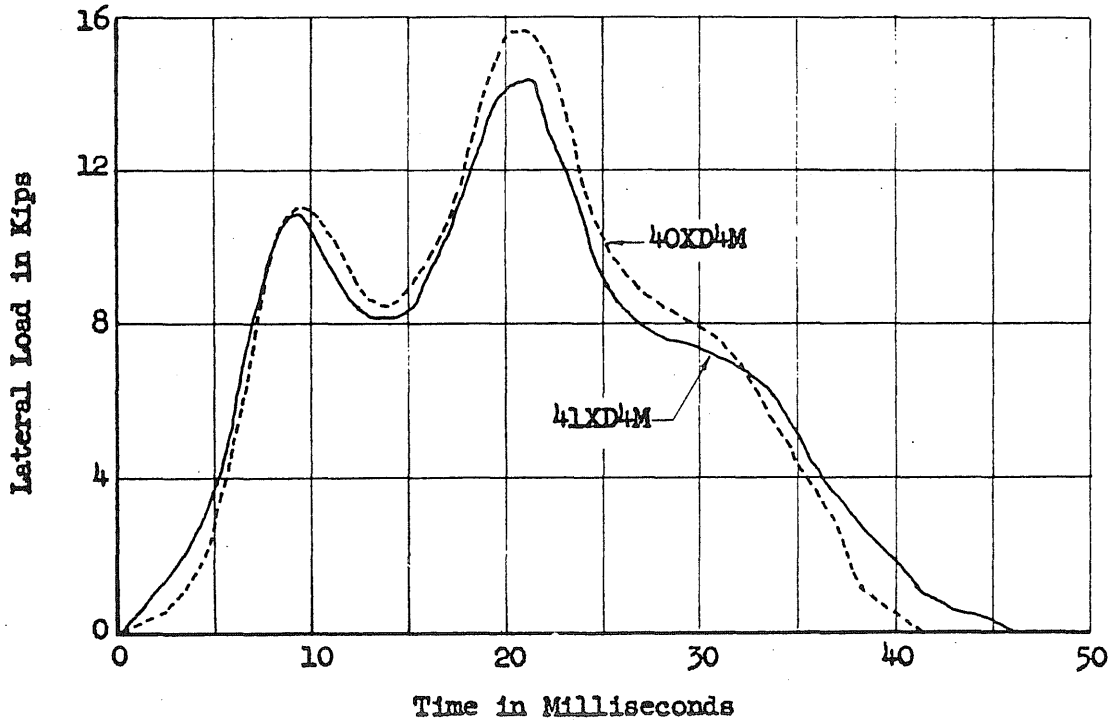

FIG. 18 LOAD-TIME RELATIONSHIP FOR STRONG DIRECTION SPECIMENS; HEIGHT OF DROP = 24 in.

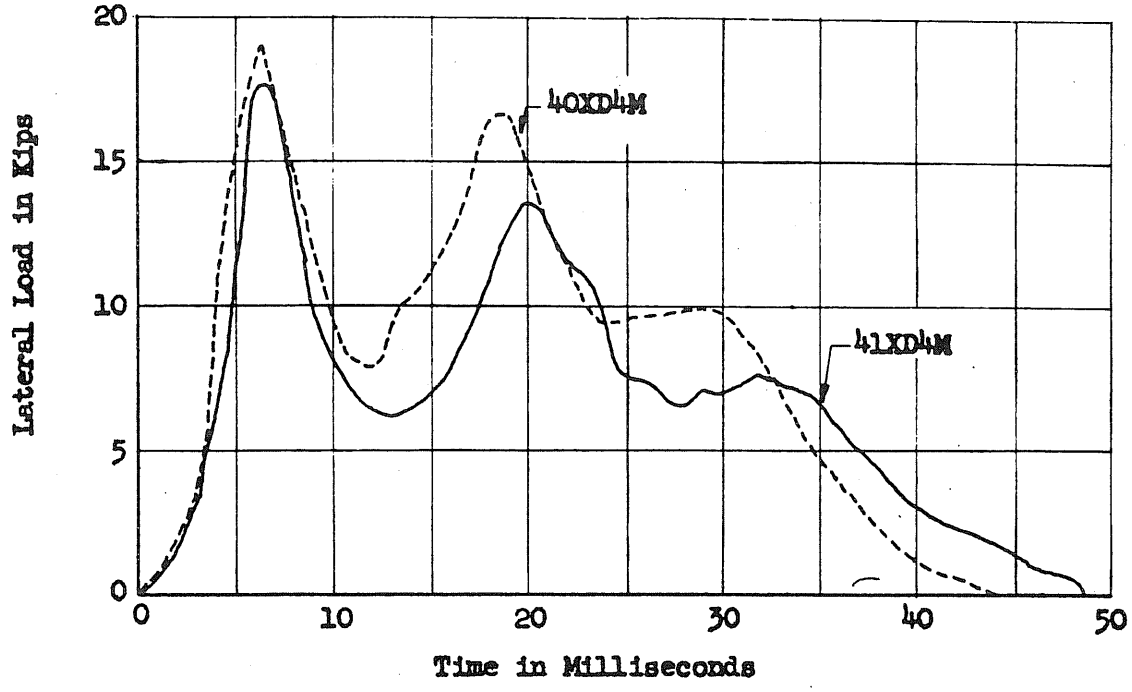

FIG. 19 LOAD-TIME RELATIONSHIPS FOR STRONG DIRECTION SPECIMENS; HEIGHT OF DROP = 48 in.

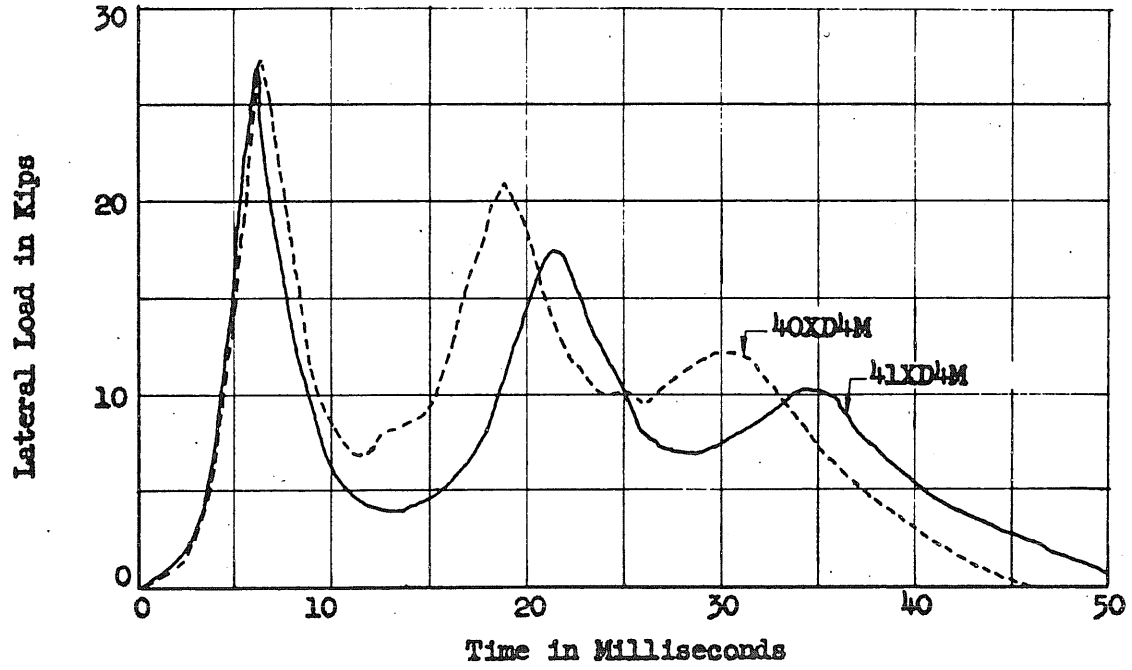

FIG. 20 LOAD-TIME RELATIONSHIPS FOR STRONG DIRECTION SPECIMENS; HEIGHT OF DROP = 72 in.

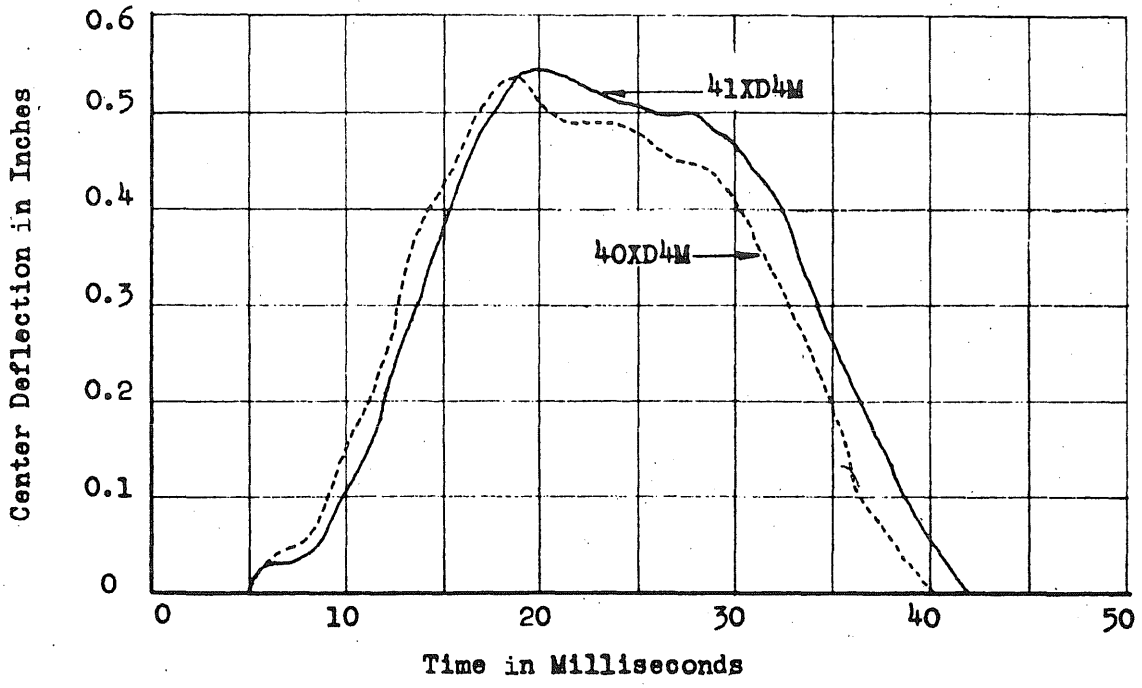

FIG. 21 DEFLECTION-TIME RESLATIONSHIPS FOR STRONG DIRECTION SPECIMENS; HEIGHT OF DROP = 12 in.

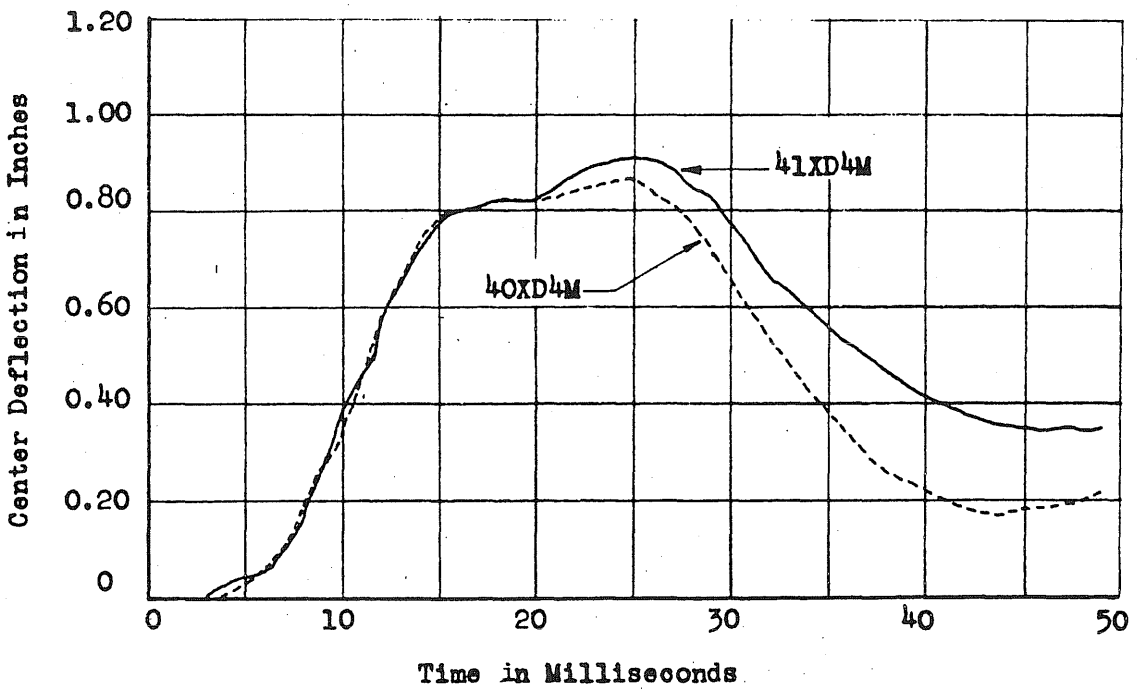

FIG. 22 DEFLECTION-TIME RELATIONSHIPS FOR STRONG DIRECTION SPECIMENS; HEIGHT OF DROP = 24 in.

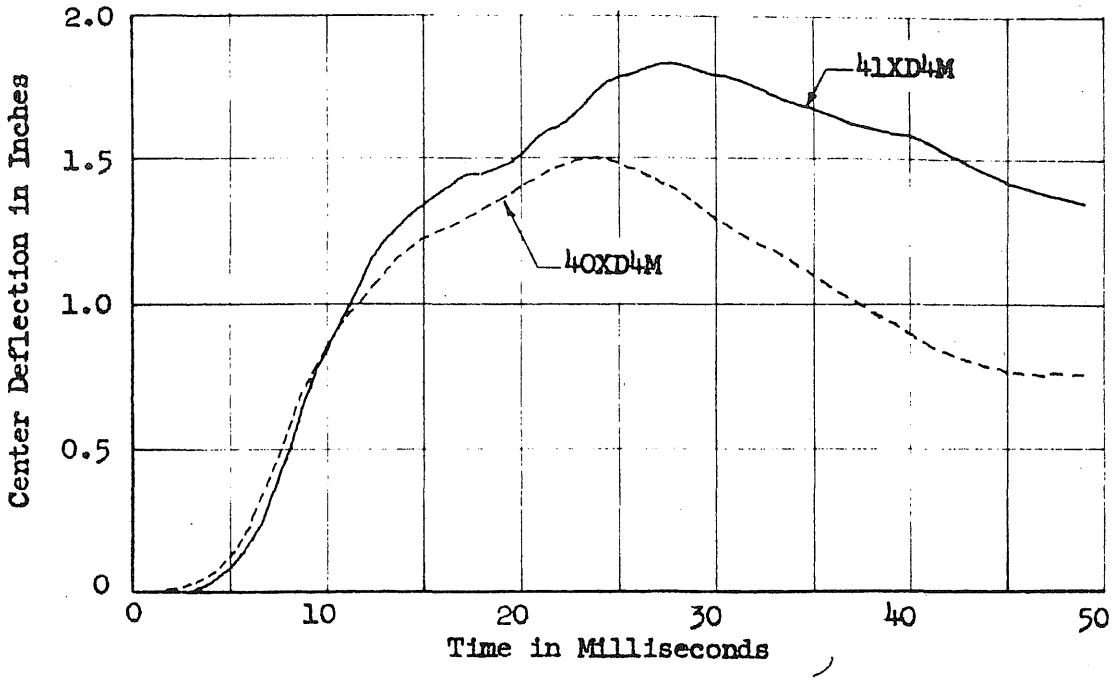

FIG. 23 DEFLECTION-TIME RELATIONSHIPS FOR STRONG DIRECTION SPECIMENS; HEIGHT OF DROP = 48 in.

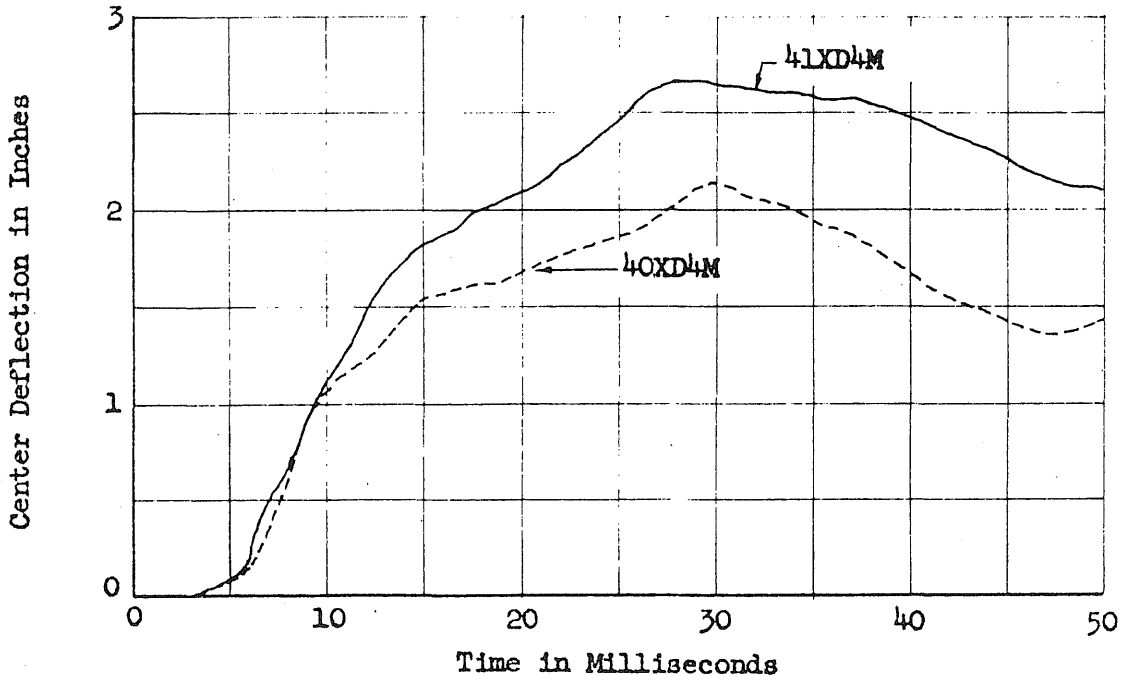

FIG. 24 DEFLECTION-TIME RELATIONSHIPS FOR STRONG DIRECTION SPECIMENS; HEIGHT OF DROP = 72 in.

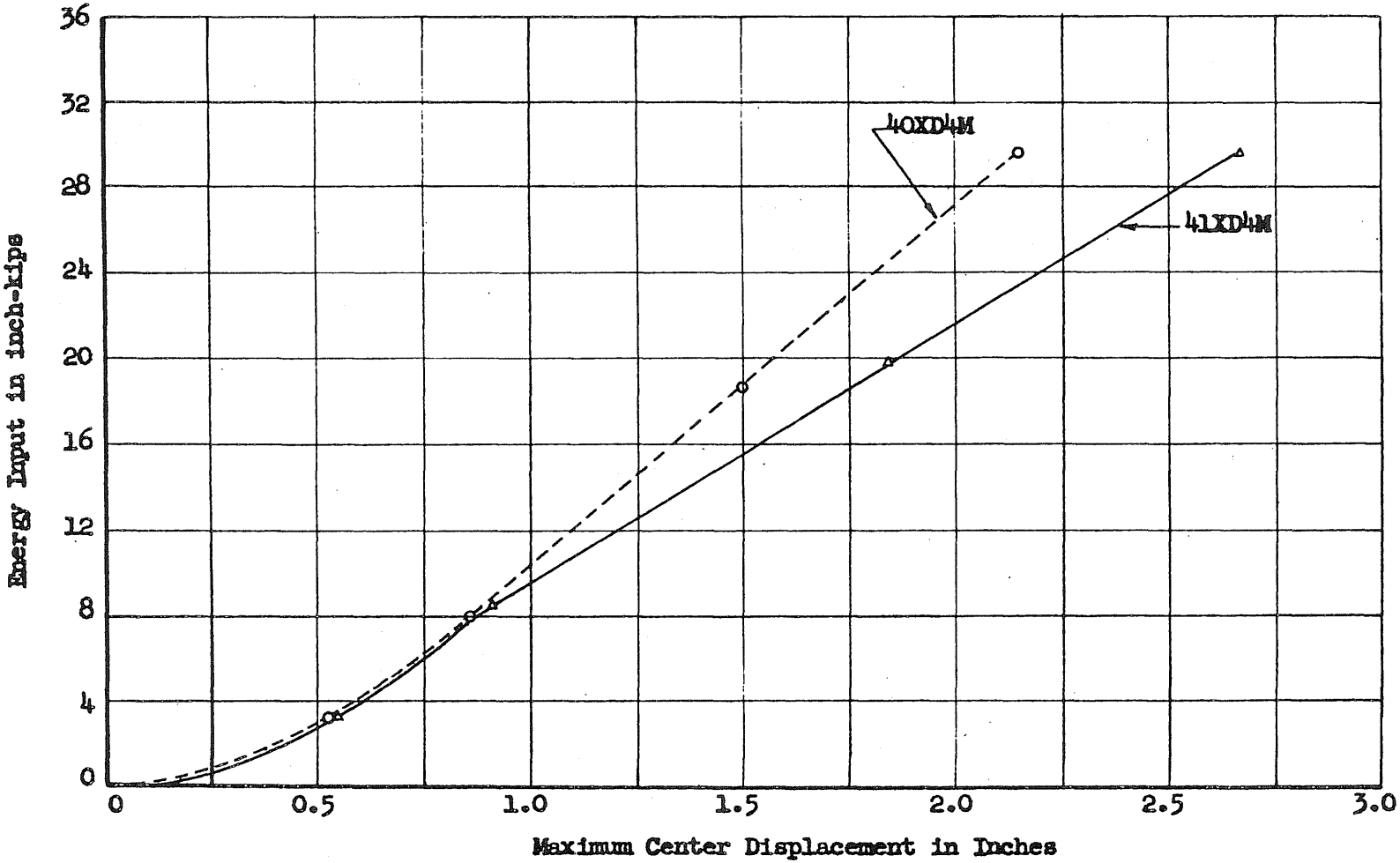

FIG. 25 TEST RESULTS OF ENERGY INPUT - CENTER DISPLACEMENT CURVES FOR STRONG DIRECTION SPECIMENS

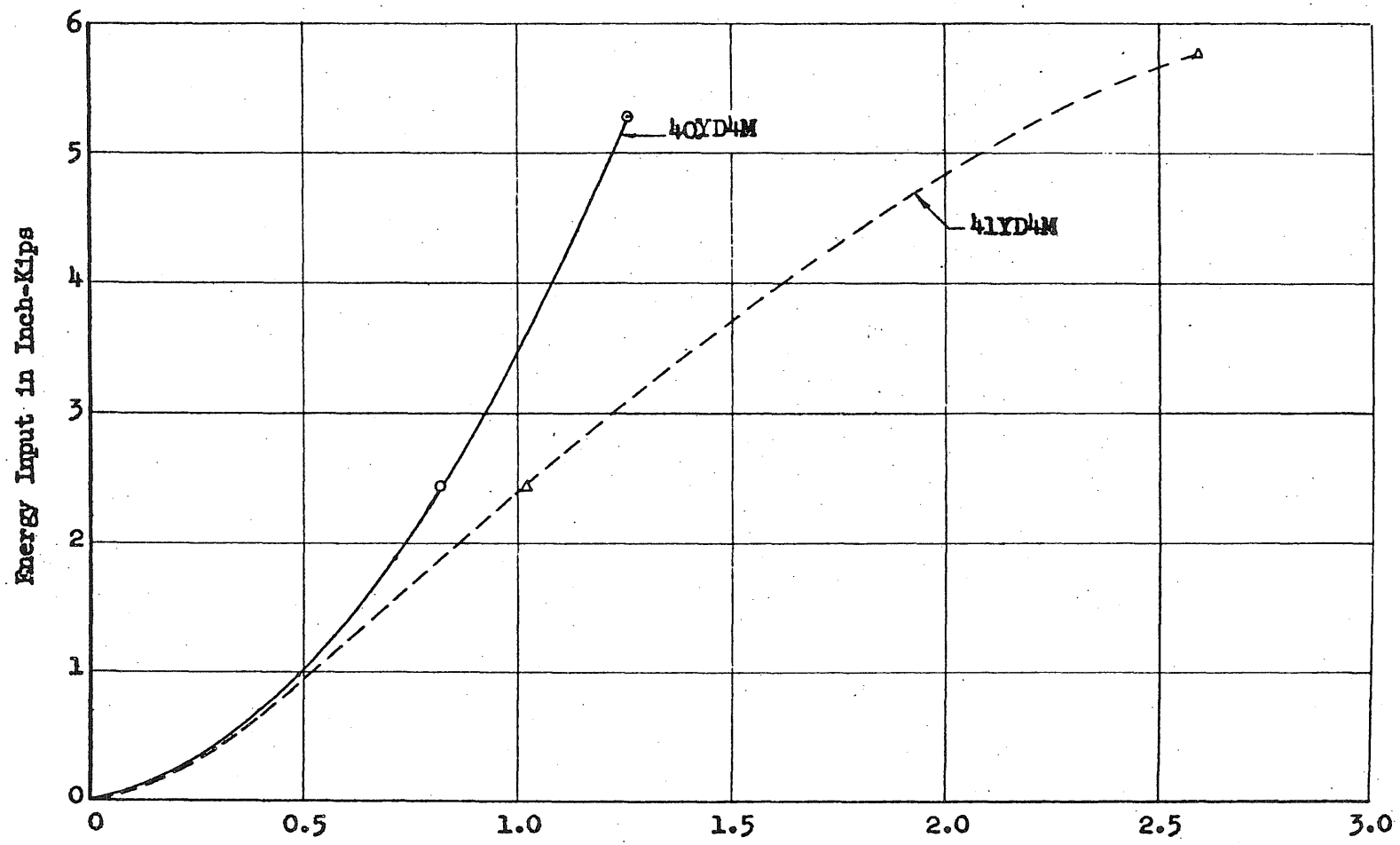

FIG. 26 TEST RESULTS OF ENERGY INPUT - MAXIMUM CENTER DISPLACEMENT CURVES FOR WEAK DIRECTION SPECIMENS

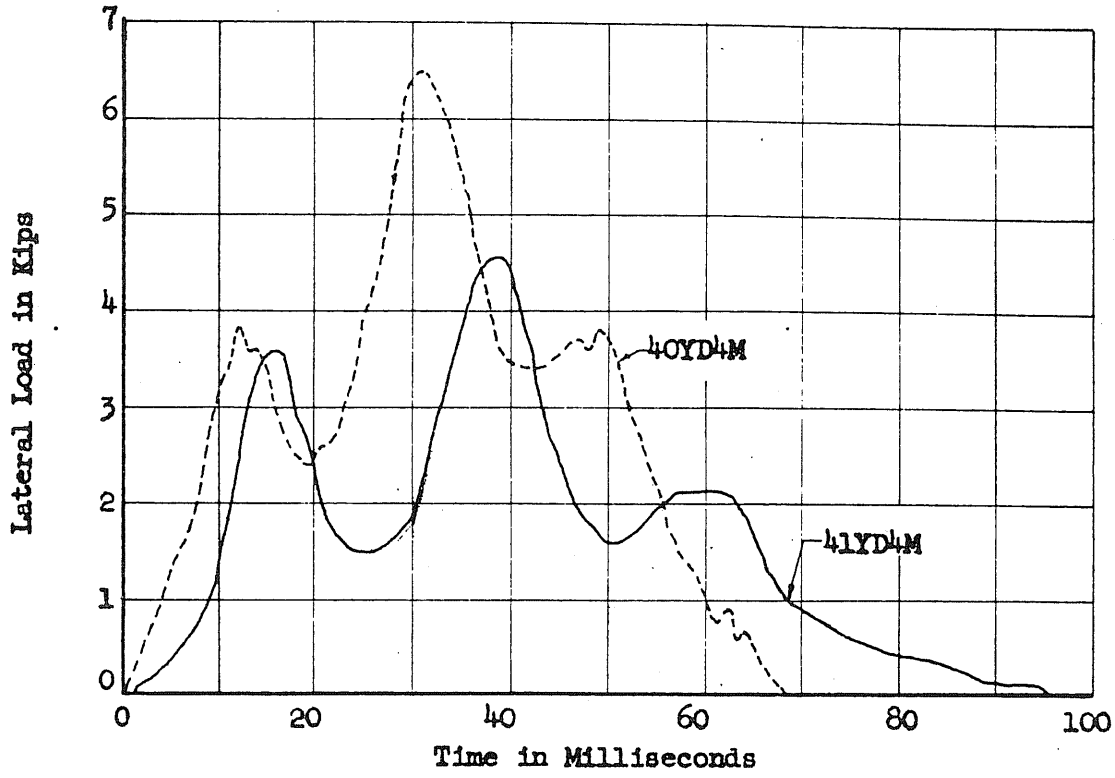

FIG. 27 LOAD-TIME RELATIONSHIPS FOR WEAK DIRECTION SPECIMENS; HEIGHT OF DROP = 6 in.

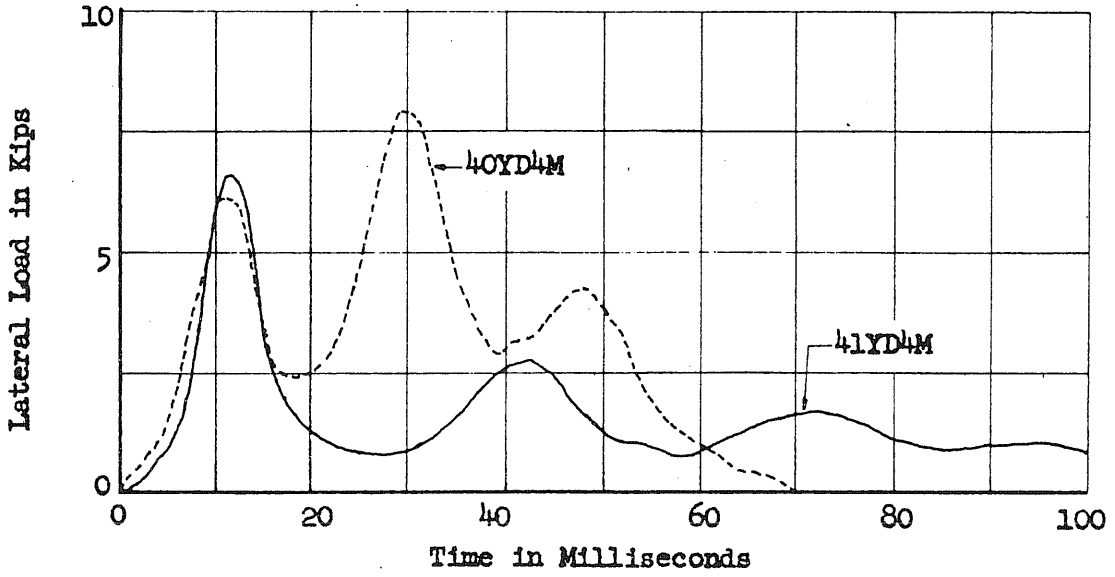

FIG. 28 LOAD-TIME RELATIONSHIPS FOR WEAK DIRECTION SPECIMENS; HEIGHT OF DROP = 12 in.

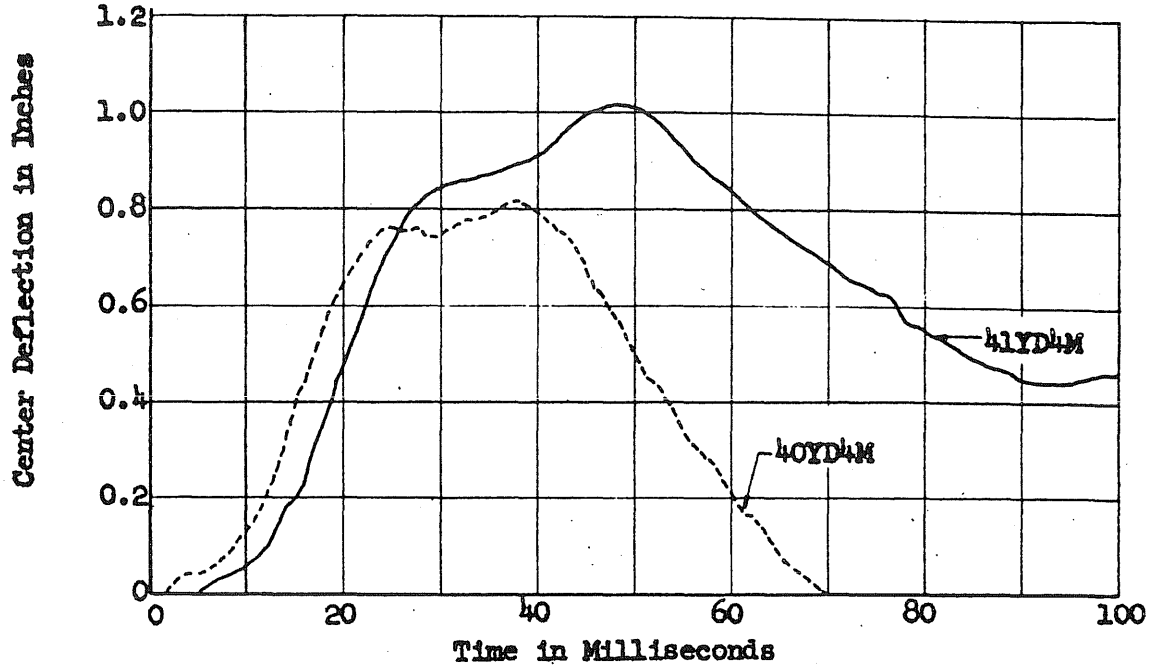

FIG. 29 DEFLECTION-TIME RELATIONSHIPS FOR WEAK DIRECTION SPECIMENS; HEIGHT OF DROP = 6 in.

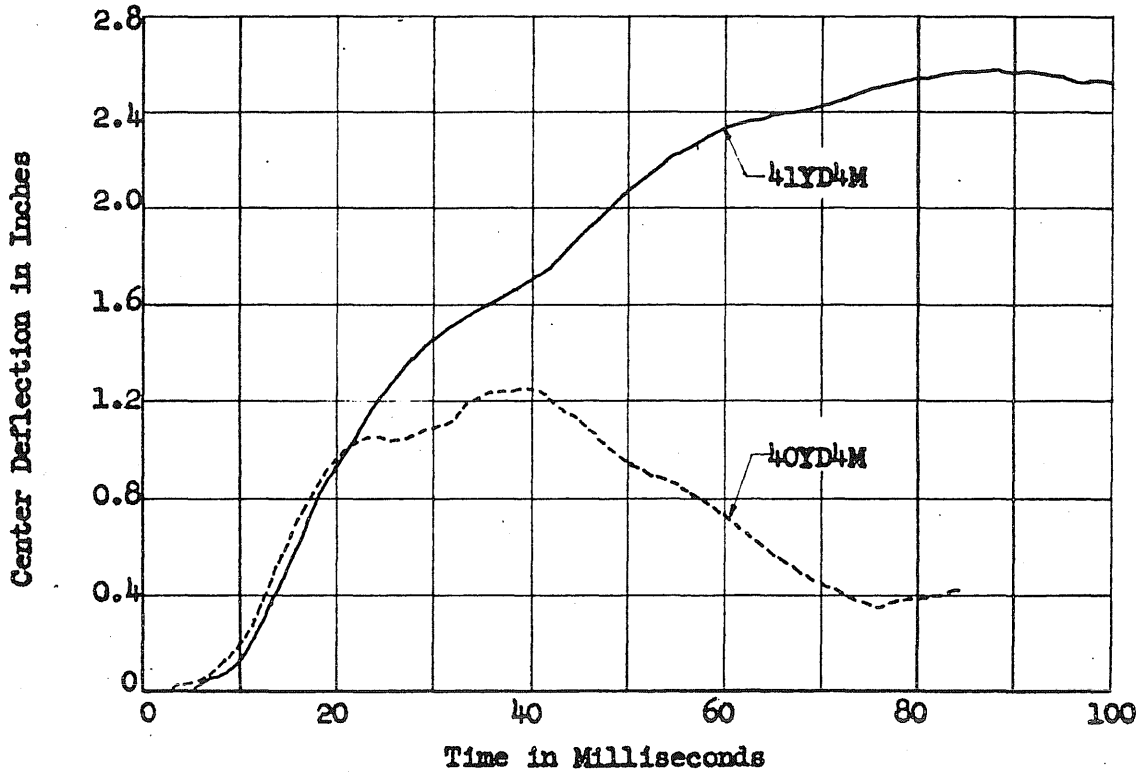

FIG. 30 DEFLECTION-TIME RELATIONSHIPS FOR WEAK DIRECTION SPECIMENS; HEIGHT OF DROP = 12 in.

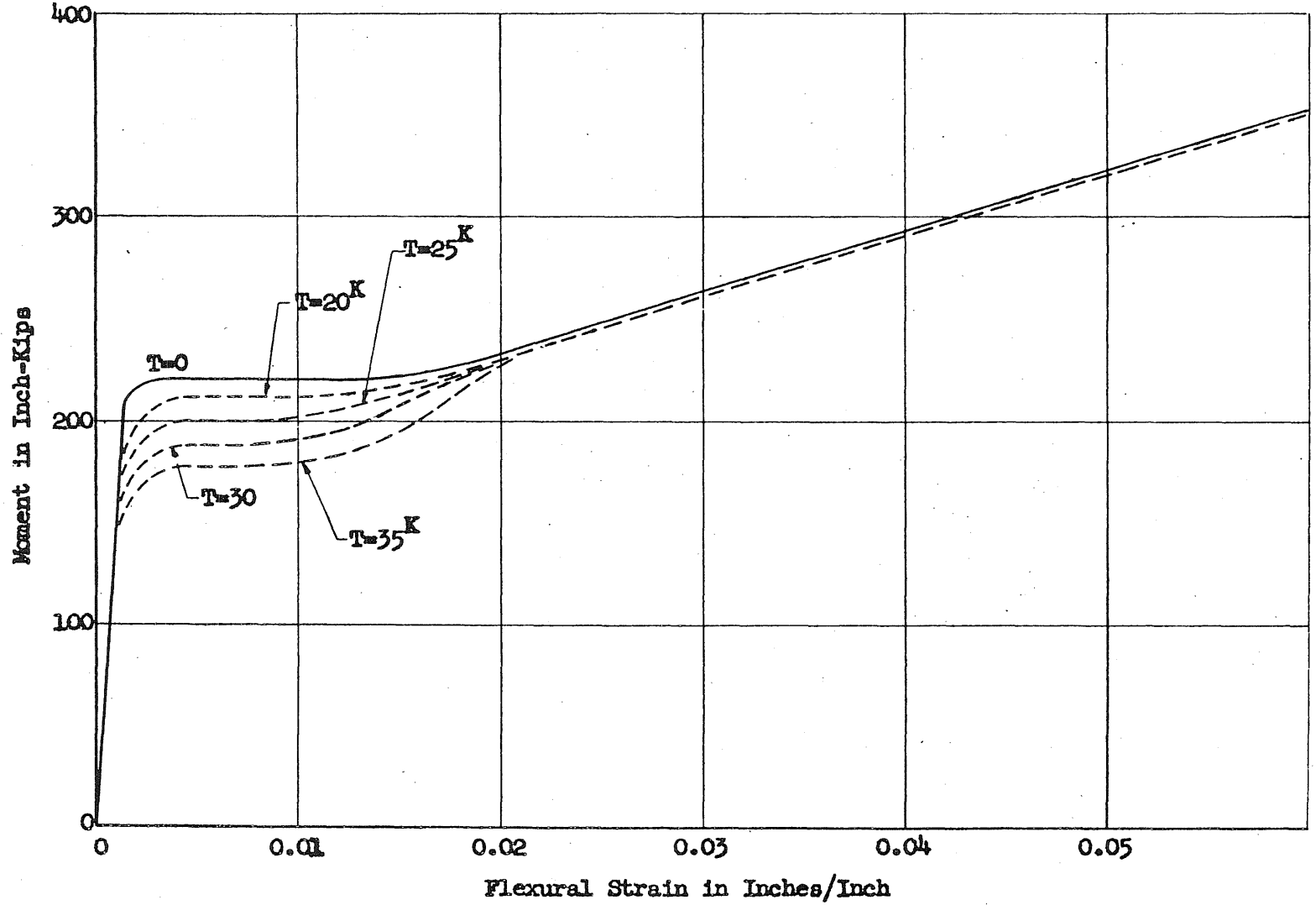

FIG. 31 THEORETICAL MOMENT-FLEXURAL STRAIN CURVES FOR SPECIMENS TESTED IN THE STRONG DIRECTION OF RESISTANCE

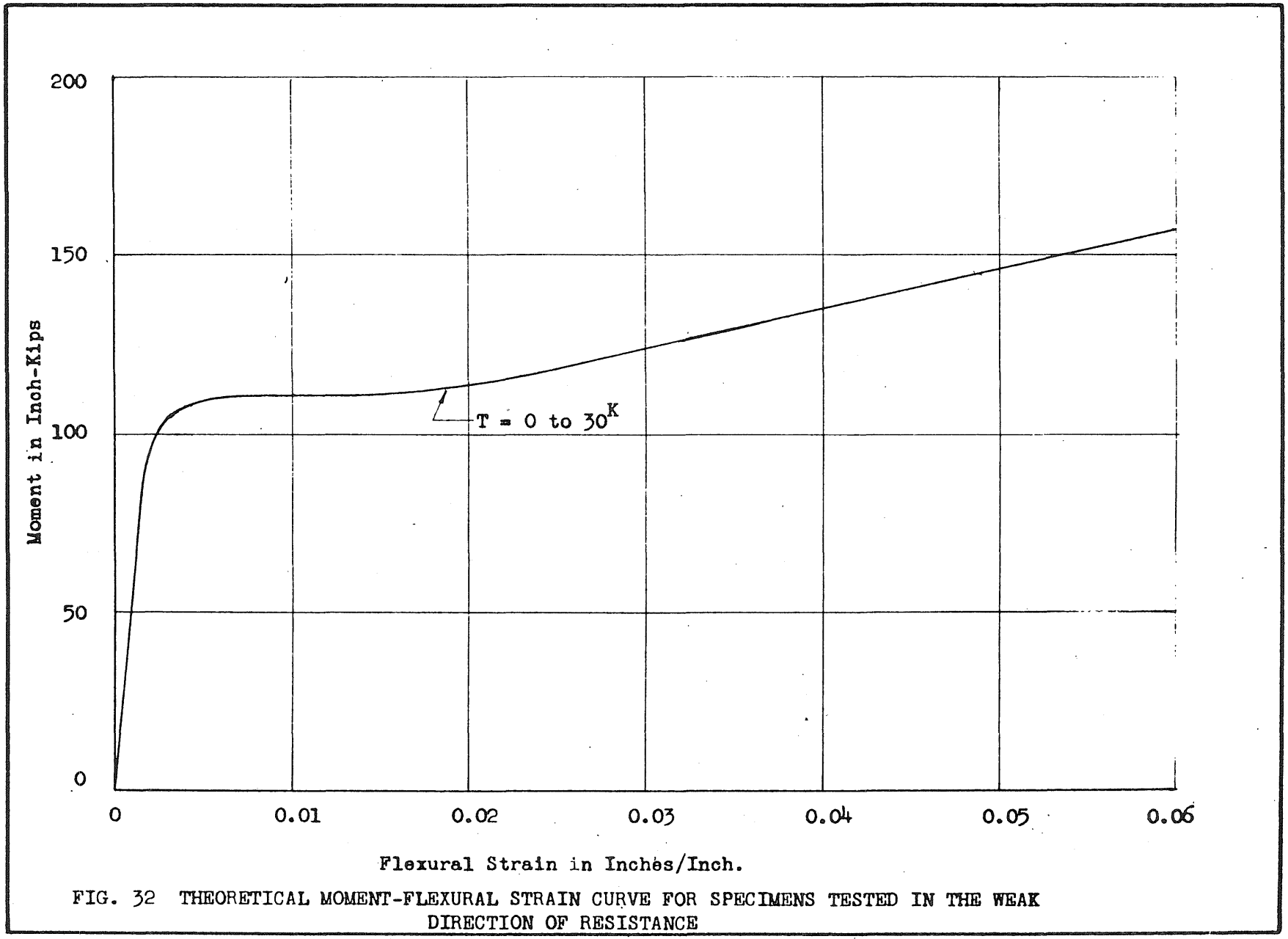

FIG. 32 THEORETICAL MOMENT-FLEXURAL STRAIN CURVE FOR SPECIMENS TESTED IN THE WEAK DIRECTION OF RESISTANCE

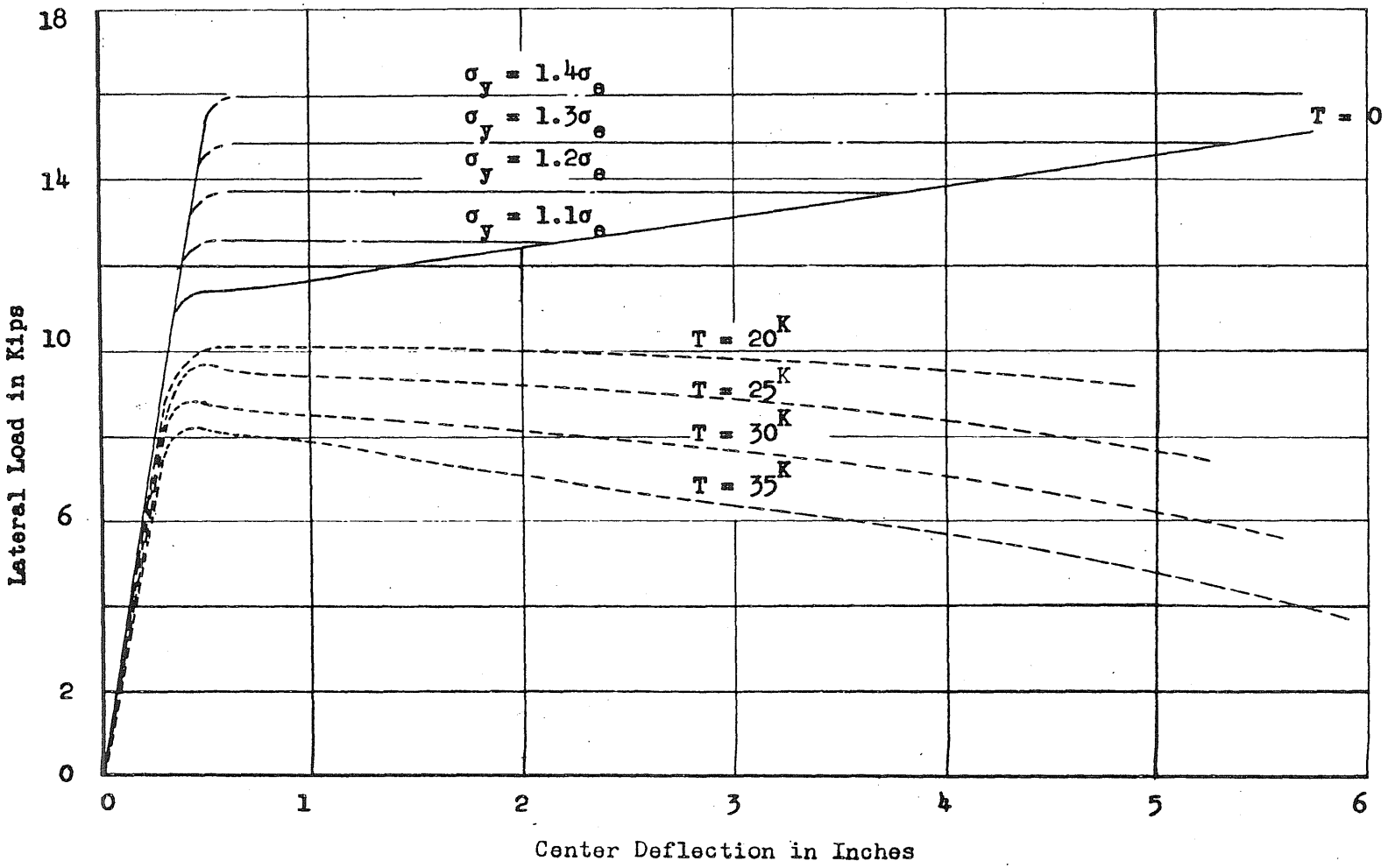

FIG. 33 THEORETICAL LOAD-DEFLECTION CURVES FOR SPECIMENS LOADED IN THE STRONG DIRECTION

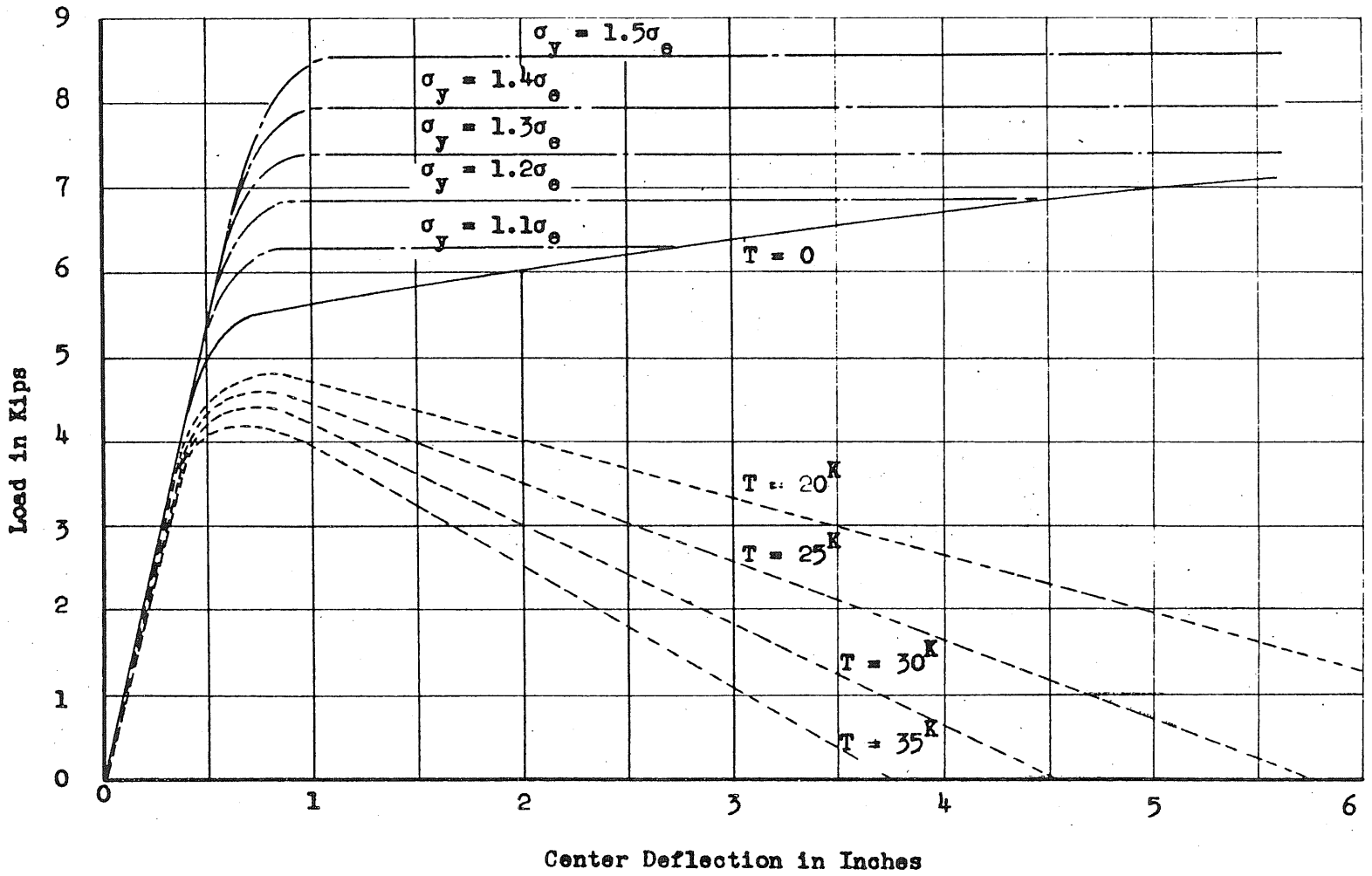

FIG. 34 THEORETICAL LOAD-DEFLECTION CURVES FOR SPECIMENS LOADED IN THE WEAK DIRECTION

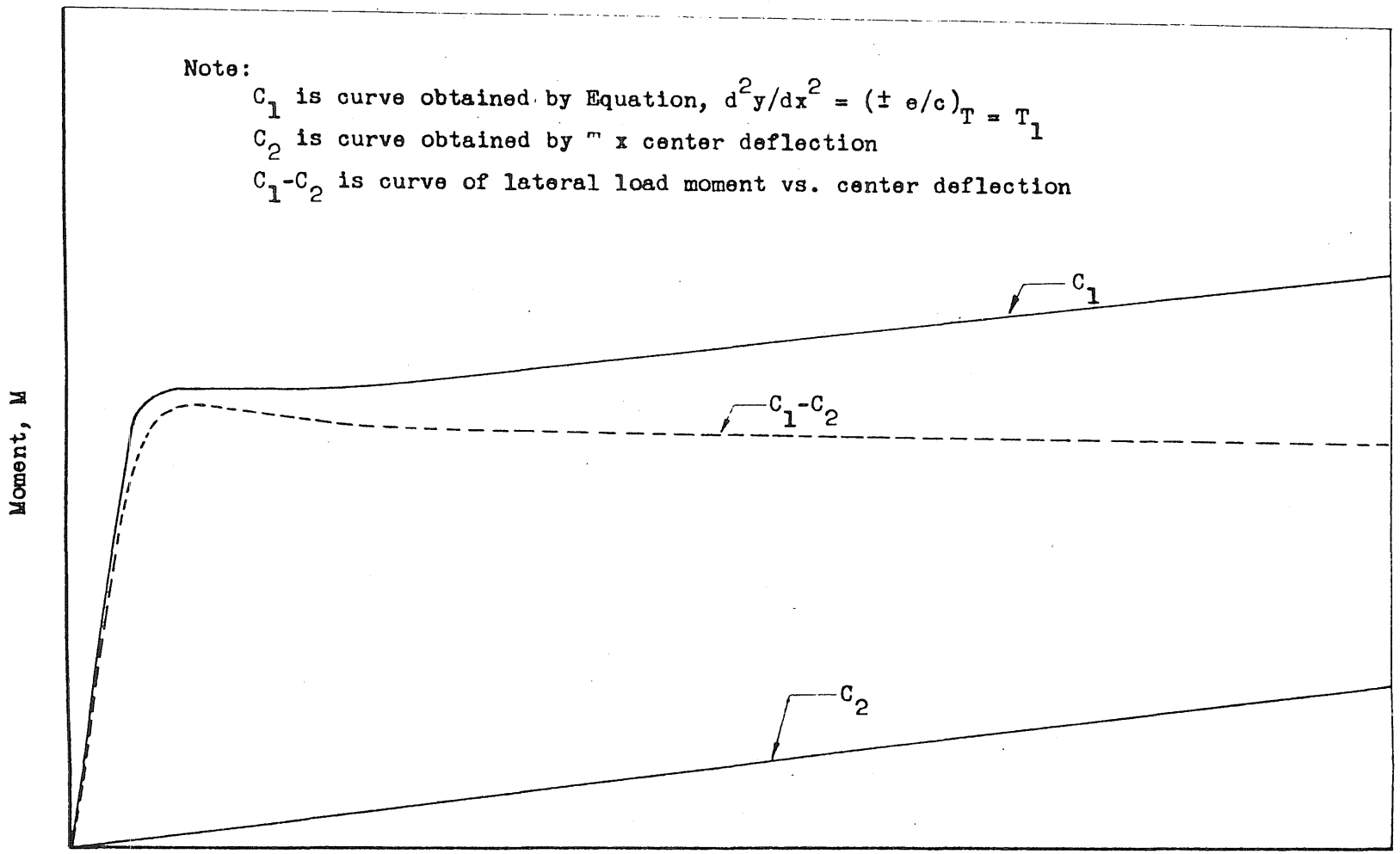

FIG. 35 GRAPHIC REPRESENTATION OF DETERMINATION OF THEORETICAL MOMENT-CENTER DEFLECTION CURVE WHEN THRUST IS PRESENT

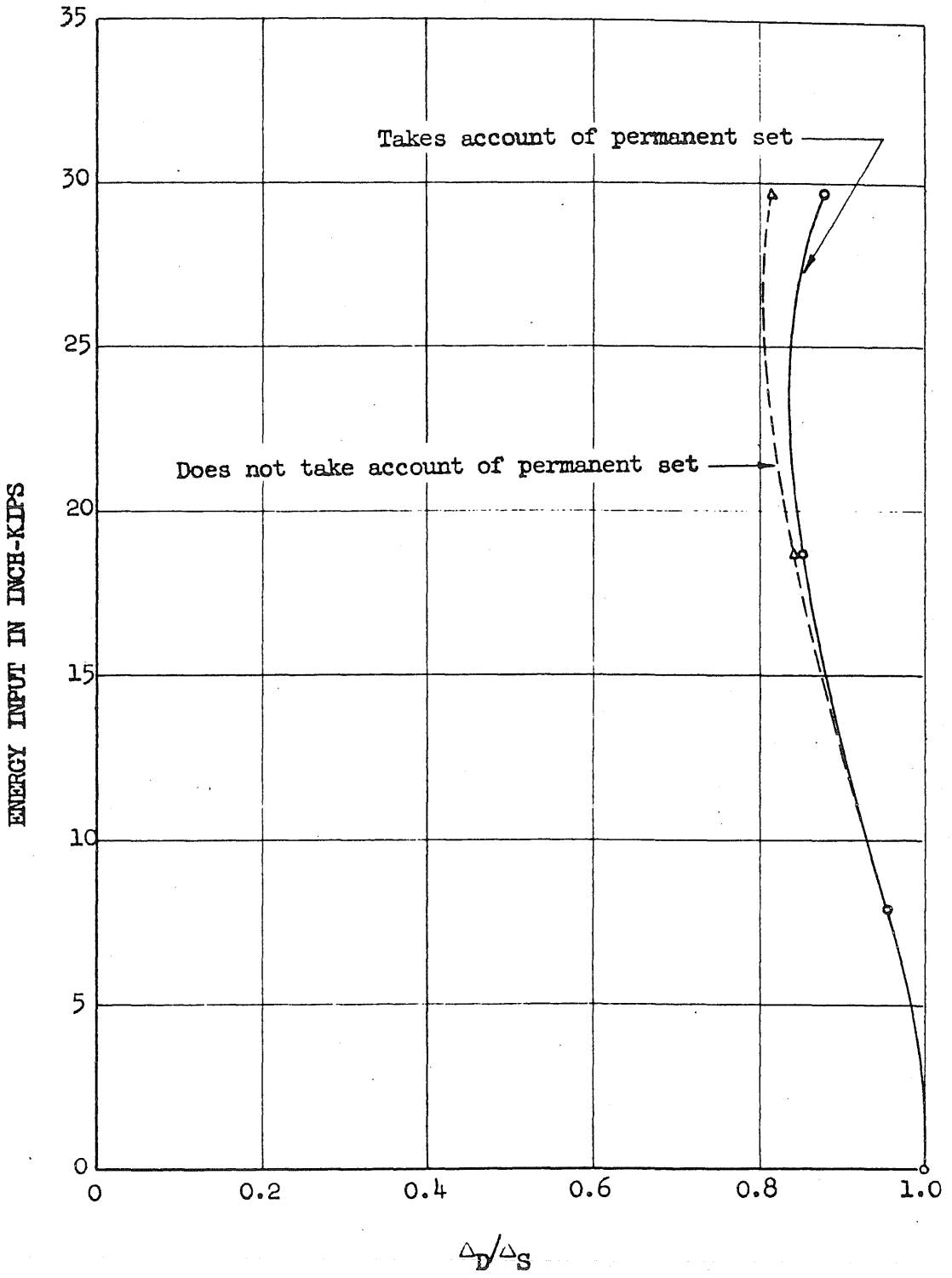

FIG. 36 ENERGY INPUT VS Δ_D/Δ_S FOR 40XD4M BASED ON TEST RESULTS AND THEORETICAL STATIC LOAD-DEFLECTION CURVE

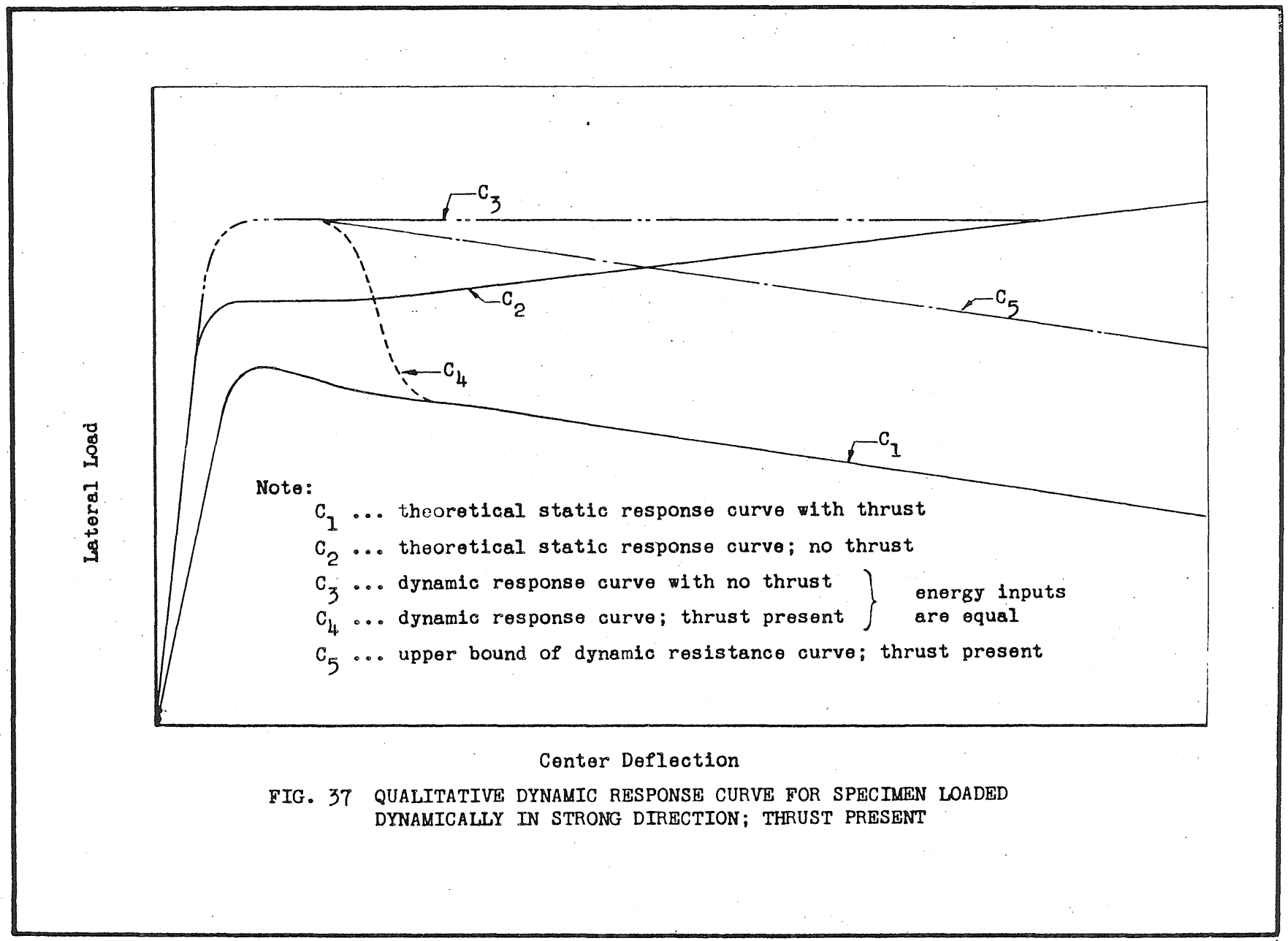

FIG. 37 QUALITATIVE DYNAMIC RESPONSE CURVE FOR SPECIMEN LOADED DYNAMICALLY IN STRONG DIRECTION; THRUST PRESENT

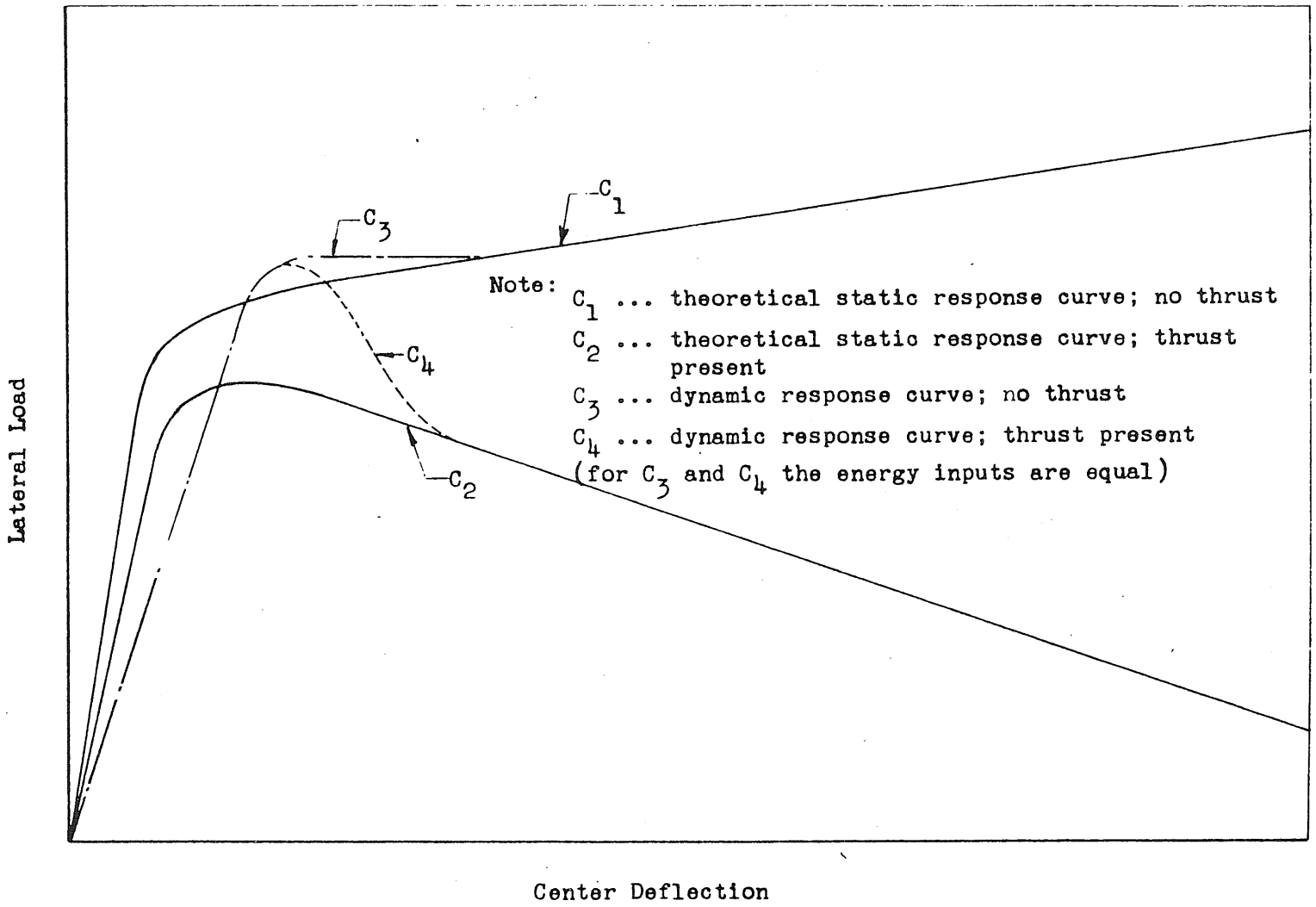

FIG. 38 QUALITATIVE DYNAMIC RESPONSE CURVE FOR SPECIMEN LOADED DYNAMICALLY IN THE WEAK DIRECTION; THRUST PRESENT